CO2 laser interactions with wood tissues during single pulse laser-incision

Nath, Subhasisa; Waugh, David ; Ormondroyd, Graham; Spear, Morwenna; Pitman , Andrew; Sahoo, Seshadev; Curling, Simon; Mason, Paul

Optics and Laser Technology

DOI:
10.1016/j.optlastec.2020.106069

Published: 01/06/2020

Peer reviewed version

CO_2 laser interactions with wood tissues during single pulse laser-incision

Subhasisa Nath[1], David G. Waugh[1], Graham A. Ormondroyd[2], Morwenna J. Spear[2], Andy J. Pitman[3], Seshadev Sahoo[4], Simon F. Curling[2], Paul Mason[5]
[1]*School of Mechanical, Automotive and Aerospace Engineering, Coventry University, Gulson Road, Coventry, CV1 2JH, United Kingdom*
[2]*The Biocomposites Centre, Bangor University, Bangor, LL57 2UW, United Kingdom*
[3]*LIGNIA Wood Company Limited, Unit 10, Atlantic Trading Estate, Barry, CF63 3RF, United Kingdom*
[4]*Department of Mechanical Engineering, Siksha "O" Anusandhan University, Bhubaneswar, 751030, India*
[5]*Millennium Lasers Limited, Units 3-5, Llan Coed Court, Coed Darcy, Llandarcy, Neath, SA10 6FG, United Kingdom*

**Corresponding author:* subhasisa.nath@coventry.ac.uk

Abstract

Incising is a technique used to improve fluid flow in impermeable woods during wood treatment processes. Previous studies relating to the laser-incision of wood have neglected many aspects such as detailed analysis of the anatomy of the wood, including consideration of tangential/radial faces and earlywood/latewood interactions with the laser beam. By considering wood anatomy, a complete investigation of the CO_2 laser-incision processes is presented that yields new knowledge of laser beam interaction with growth rings when incising into tangential/radial faces, and the low-density earlywood and higher density latewood within the growth ring. Southern Yellow Pine, Radiata Pine, European Redwood and Beech, each having different bulk densities, were laser-incised using a 2 kW ROFIN CO_2 laser with radiation in the far-infrared regime (10.6 μm). Microstructural characterisations were carried out to better understand the effect of CO_2 laser-incision and its parameters on the depth, diameter and quality of the incised holes. The laser-incised hole shapes were found to be uniform in depth, however, the hole circularity was significantly affected by the presence of earlywood and latewood tissues. Maximum and minimum diameters of incised holes were measured in the Radiata Pine (~ 1.3 mm) and in the Beech (~ 0.7 mm), respectively.

Similarly, for equal laser powers used, the maximum and minimum depths of laser-incised holes were measured in the European Redwood (~ 33 mm) and in the Beech (~ 25 mm), respectively, with the laser incident on the radial face of the samples. CO_2 laser pulse duration had a greater effect on diameter and depth of incised holes when compared to laser power and showed that the CO_2 laser pulse duration is a dominant parameter when designing CO_2 laser-incision processes.

Keywords: Laser-incision; CO_2 laser; wood; depth; diameter; circularity

1. Introduction

Preservative treatment of less durable timbers requires fluids to penetrate the wood to a sufficient depth in order to protect the wood from attack by fungi, insects and marine borers. This is important where wood will be used in applications that leave it more susceptible to fungi, insects and marine borers. These applications are predominantly for exterior applications such as window joinery, fencing and cladding, as well as structural elements in buildings and bridges [1-3]. As would be expected, further protection of wood through preservative treatment is required for wooden structures located outdoors and usually where longer material usage lives are required. The effectiveness of preservative treatment is determined by its penetration and retention [4]. Permeability of the wood species influences preservative penetration and retention, as many wood species and regions of its structure (i.e. heartwood) are impermeable. On account of this, it is imperative that the wood preservative treatment industry have sufficient strategies and techniques to ensure that efficient and effective impregnation of fluids into wood is carried out.

There have been several methods used to improve wood permeability, including incising (by mechanical processes, or to a lesser extent laser), steaming, solvent-exchange drying, critical point drying and biological treatments [5]. Out of these techniques, mechanical incising methods have, to date, proven most effective to assist in the lateral permeability of wood [5]. The process tends to produce millimetre scale holes/slits in the wood, to several millimetres in depth for preservative penetration [6]. Whilst mechanical incisions have been shown to be effective for enhancing preservative treatment processes, the technique is limited in the fact that small holes or complex incision geometries are either hard or impossible to achieve. In addition to this, several millimetres of penetration from mechanical incision severely limits the thickness of wood that can be incised and then treated with preservative, often resulting in an 'envelope treatment' rather than full impregnation. Laser-incision is a technique which could eradicate these issues as it would allow the creation of finer incisions, the development of more complex incision patterns and give rise to deeper incision holes, when compared to mechanical incision technologies.

Lasers are frequently used for cutting and drilling of metallic and non-metallic materials, including composites, due to their superior performance against conventional machining processes [7-10]. The use of lasers for wood processing were initially meant only for cutting, marking and engraving [11-13]. Initially, it was thought that laser-incising was not economically viable [14]. However, with the further development of laser technologies it has recently been concluded that laser-incising is an efficient technique to create narrow, deep holes for preservative treatment [15-20]. Although, it has been reported that laser-incision of wood can lead to the formation of a heat affected zone (HAZ), carbonisation and loss of mechanical strength [21-25]. The formation of

the HAZ, and carbonisation was found to result from thermal decomposition of the wood structure after laser-incision and has been explained by the chemical constituents of the wood decomposing over the range 170–260 °C for hemicelluloses, 240–350 °C for cellulose and 280–550 °C lignin [22]. Wang *et al.* [22] also used a 1 kW laser with pulse durations ranging from 50 to 300 ms which increased the exposure time of wood to the laser irradiation, thereby forming the HAZ. It has been shown that the HAZ can be controlled using a shorter laser pulse duration [23, 24], highlighting the importance of the laser pulse duration on the laser-incision process, and potential for optimisation.

It has been reported that the strength of lumber decreases after mechanical incision [19]. In a similar manner, it has been shown that the formation of the HAZ during laser processing of wood was reported to affect the tensile strength of wood [23, 25]. Because of this, the control of the HAZ could be deemed an important aspect that needs to be considered during the design and implementation of wood laser-incision. This further highlights the potential importance of the laser pulse duration for laser-incising of wood. Kortsalioudakis *et al.* [25] investigated the effect of laser incision on the strength of the wood. It was found that when using a Nd:YAG laser operating at 532 nm wavelength and with a laser energy greater than 70% of maximum energy, carbonisation was present. However, it was shown that this did not negatively affect the strength of the incised woods. Previous studies on CO_2 laser-incising have used high-powers and long pulse durations which were believed to be critical in destroying the structural materials of the wood cells [21-24, 26-29]. Panzer *et al.* [21] investigated the effect of excimer lasers and CO_2 lasers on the laser ablation efficiency and structural change associated with it. They found that the use of CO_2 laser and higher energy density increased the ablation efficiency and increased damage to wood structure.

However, the use of an excimer laser led to significantly less damage of the wood structure. The use of high-power during laser processing of wood resulted in melting and formation of wood charcoal on the surface of the wood [29, 30]. Wang *et al.* [22] found that the lignin decomposition and deposition of residue were evident following laser-incision of wood with the CO_2 operating at an output power 1 kW and a pulse duration of 300 ms. Barcikowski *et al.* [23] reported significant thermal decomposition/pyrolysis of lignin at the cell wall of wood structure following laser cutting. All these studies, whilst reporting on the strength of the laser-incised wood species, do not necessarily fully account for the importance of the pulse duration. These works are also limited in the discussion surrounding the laser interactions with growth rings, i.e. the earlywood and latewood tissues, and how these impact upon the laser-incision process. Furthermore, these studies were unable to explain the microstructural changes that occurred following laser-incision and the parametric effect of laser-incision on incised hole shape, size and quality.

Understanding the incising efficiency of a CO_2 laser and its associated effects on wood are the primary objectives of the present work. CO_2 laser-incising was performed to understand its effect on shape, size, depth and quality of incised holes. The effect of the CO_2 laser on different wood species was also investigated to achieve a better understanding of the driving laser parameters for the laser-incision of wood. A detailed analysis of laser-incised holes has been undertaken to better understand the level of laser-induced damage to the wood structure and subsequently, understand the mechanism of laser-incision. From this, the importance of pulse duration during CO_2 laser-incision is evidenced and discussed for the first time. Furthermore, this work

evidences and discusses the importance of the laser interaction with earlywood and latewood during CO_2 laser incision processes.

2. Experimental Technique

2.1 Materials

In the present study, four different wood species were used (Southern Yellow Pine, Radiata Pine, European Redwood and Beech). These were selected to represent different levels of permeability and potential for enhancement by laser incision. Each wood was used as supplied. The air-dry density and moisture content were measured gravimetrically according to BS EN 13183-1:2002 for small samples cut from the supplied plank. The schematic diagram of wooden blocks, used for the laser-incision, is shown in Figure 1. The wooden blocks were machined to a dimension of 100 mm ×35 mm × 30 mm from large pieces and had a fine sawn finish.

The details of the wood species used in the present study are presented in Table 1. It is to be mentioned here that Southern Yellow Pine, Radiata Pine and European Redwood are different species of pine, and are classified as softwoods, whereas Beech is the densest among the studied wood species and is classified as a hardwood. In the European Redwood, which was sourced from mainland Europe via a timber merchant, the number of growth rings (i.e. bands of earlywood and latewood) per centimetre was the highest among the pines studied.

The specific heat capacity and thermal conductivity of the different wood species were calculated at room temperature (25 °C) according to Equation (1) and Equation (2) and are given in Table 1 [31].

$$c_p = \left(\frac{c_{po}+0.01\,MC\,c_{pw}}{1+0.01MC}\right) + \mathrm{B} \qquad (1)$$

$$k = 0.0238 + \frac{(0.2005+0.004039MC)\rho}{1000(1+0.01MC)} \quad (2)$$

where, c_{po} is the specific heat of dry wood at room temperature (≈1.21 kJ/kg K), c_{pw} is the specific heat of water (≈ 4.187 kJ/kg K), MC is the moisture content (%), B is the additional specific heat due to wood-water bond energy (≈ 0.084 kJ/kg K), k is the thermal conductivity (W/m K) and ρ is the density (kg/m^3).

2.2 Laser-incisions

A 2 kW CO_2 laser (Rofin Sinar, UK) was used to carry out the laser-incisions. The schematic of the laser-incision process set-up is shown in Figure 2. Laser-incisions were made in the radial and tangential faces of the Southern Yellow Pine, Radiata Pine, European Redwood and Beech, to establish how the growth rings influenced incision efficiency as wood is anisotropic in nature as shown in Figure 1. The laser incisions were carried out with a radiation wavelength of 10.6 μm and a single-pulse laser incision strategy was employed. A single-pulse laser incision implies irradiating the wood surface once with a single pulse of pre-defined laser power and pulse duration. The laser powers used for laser incision were 1% (calibrated to 70 W), 3% (calibrated to 80 W), 5% (calibrated to 100 W), and 10% (calibrated to 170 W). The laser pulse durations at each laser power were changed from 1 ms to 80 ms during laser incision experiments to determine the effects on incision efficiency and hole characteristics. The laser pulse frequency was kept constant at 1 Hz during the laser-incision experiments. The CO_2 laser had a Gaussian distribution of intensity with an M^2≈1.05. The parameters used for laser-incision are presented in Table 2. The CO_2 laser raw beam diameter was 20 mm and was focussed down to 0.3 mm using a fused silica lens with a focal length

of 127 mm. The focused laser beam diameter with a lens of focal length of 190 mm was 0.37 mm. No processing assist gas was used during laser-incision study to reduce any additional heat input or temperature fluctuations due to exothermic reactions.

The theoretical laser beam radius at focus was calculated according to Equation (3).

$$R_f = \frac{1}{\pi}\frac{f\lambda}{R_0} \quad (3)$$

where, R_f is the beam radius at focus (mm), f is the focal length of lens (mm), λ is the wavelength of the laser beam and R_0 is the raw beam radius (mm).

The depth of focus was calculated according to Equation (4).

$$z_f = \frac{\pi \times R_f^2}{\lambda} \quad (4)$$

where, z_f is the depth of focus (mm), R_f is the radius of the beam at focus (mm), and λ is the wavelength of the laser beam.

The wood specimens were placed perpendicular to the laser beam as shown in Figure 2. Five holes were incised into each wood sample using the CO_2 laser with each laser power and pulse duration combination.

2.3 Hole shape and size analysis

Following laser incision, optical microscopy (Axio Observer; ZEISS) was used to measure the hole diameter and hole depth for each of the wood specimens. To measure the depth of CO_2 laser-incised holes, a sander was used to prepare the cross-sections following which a compressed air jet was used to clean any residue left due to sanding. Prior to microstructural analysis the wood samples were oven dried for 2 hours at 50 °C to remove moisture following which the samples were sputter coated with gold-palladium mixture for 180 seconds. Samples prepared for the depth measurements were also observed using field emission scanning electron microscope (Gemini FESEM;

ZEISS) to provide microstructural analysis of the wood cells adjacent to the laser incised holes.

Circularity of the incised holes was determined to understand the effect of laser power and pulse duration on the degree of roundness of the laser-incised holes. The circularity of incised holes was calculated according to Equation (5):

$$Circularity = \frac{D_{min}}{D_{max}} \quad (5)$$

where, D_{min} and D_{max} represent diameter measures in the direction perpendicular to each other as shown in Figure 3.

2.4 Peak surface temperature measurement

To further understand the effect of laser irradiation on the wood structure, the resulting surface temperature from the laser irradiation, T_s, was calculated according to Equation (6) [32].

$$T_s = T_0 + \frac{I_a}{\rho c_p u_d} - \frac{L_m}{c_p} \quad (6)$$

where, T_0 is the ambient temperature (K), I_a is the absorbed laser power density (W/m^2), ρ is the bulk density of wood species (kg/m^3), c_p is the specific heat (J/kg K), u_d is the drilling speed (m/s) and L_m is the latent heat of fusion (J/kg).

2.5 Finite element analysis

A finite element simulation of heat transfer in the wood was carried out using ANSYS 19.2 platform by solving three-dimensional Fourier heat conduction equation. The model was developed to investigate the temperature distribution in the wood for a laser interaction time of 1 ms and 80 ms at a laser power 70 W and 170 W, respectively.

3. Results and discussion

3.1 Effect of laser power on the diameter of incised holes

Figure 4 shows the effects of applied laser power on the diameter of the laser-incised holes in (a, b) Southern Yellow Pine, (c, d) Radiata Pine, (e, f) European Redwood and (g, h) Beech for different laser pulse durations. The plots in Figure 4 (a, c, e, g) illustrate the effects for incisions made into the radial face and plots Figure. 4 (b, d, f, h) illustrate the effects of incisions into the tangential face. From Figure 4 (a-h), it is evident that the variation in incised hole diameter with laser power is minimal for lower laser pulse durations (1 ms to 10 ms). However, the CO_2 laser-incised hole diameter increased with laser power for longer laser pulse durations over 50 ms, as shown in Figure 4. A maximum 85 % increase in hole diameter took place when the pulse duration was changed from 1 ms to 80 ms. This is due to the increased laser power enabling a higher heat input into the wood causing enhanced melting, vaporisation and material removal. It is also evident that the laser pulse duration had a strong effect on determining the hole shape and the hole size, as the laser pulse duration defined the interaction time between the laser radiation and the wood. In the Southern Yellow Pine, the change in diameter of the laser-incised holes was not different, which implies other factors (earlywood and latewood sequence, geometries, thickness etc) are involved in controlling the diameter of CO_2 laser-incised holes in Southern Yellow Pine. Figure 5 shows schematic diagrams of some idealised CO_2 laser-incision strategies in earlywood with the CO_2 laser beam incident on the radial face (Figure 5(a)), in latewood with the CO_2 laser beam incident on the radial face (Figure 5(b)) and in earlywood and latewood with the CO_2 laser beam incident on the tangential face (Figure 5(c)). In comparison, Figure 5(d) shows a more realistic, less idealistic depiction with the CO_2 laser beam

producing incisions through growth rings which are at an angle to the incident CO_2 laser beam. This is more realistic as it is known that the growth rings within wood are not always perfectly circular as depicted by Figure 5(a), 5(b) and 5(c). In Pines and Beech the earlywood and latewood have different densities, with the latter being denser. The Southern Yellow Pine has a very pronounced difference between earlywood density and latewood density, with latewood density being on average 1.9 times higher than the earlywood value [33]. For the other species in this study the difference was less pronounced. During experimentation, the earlywood and latewood tissues were to be found positioned in different orientations within the wood's structure as depicted and demonstrated in Figure 5. The laser-incisions were broadly affected by bulk density and moisture content in wood. Having said that, it has been observed that the interaction of the laser beam with the earlywood resulted in a larger hole diameter as compared to its interaction with a latewood. In Southern Yellow Pine, the presence of earlywood and latewood tissues in the structure had a strong effect on the CO_2 laser-incised hole diameter as observed from Figure 4 (a, b). In the shorter pulse duration regime (1-10 ms), the effect of laser power on incision diameter was not significant as it is evidenced by Figure 4 (a, b). The unexpected slight change in the CO_2 laser-incised hole diameter, at 80 W, shown in Figure 4 (a, b) can be explained by the possibility of a change in laser-beam interaction as the CO_2 laser-beam transitioned into a new region of either earlywood or latewood tissue. Similarly, the unexpected slight increase in CO_2 laser-incised hole diameter at 70 W (Figure 4 (b)) in the longer pulse duration regime (50-80 ms) can be attributed to the CO_2 laser beam interacting with more earlywood tissue rather than latewood tissue. This will have given rise to the larger CO_2 laser-incision hole diameter. The effect of CO_2 laser power on the diameter of the CO_2 laser-incised holes was more significant in lower density wood (Figure 4 (c, d)) compared with the

higher density wood (Figure 4 (g, h)). It should be noted here that there was no significant difference observed in the diameter of the CO_2 laser-incised holes between those laser-incision which were made on the radial and tangential faces.

3.2 Effect of laser power on the circularity of incised holes

Figure 6 to Figure 9 show the variation in circularity of CO_2 laser-incised holes with applied laser power for Southern Yellow Pine, Radiata Pine, European Redwood and Beech, respectively. Circularity of incised holes which are close to unity is considered as better in laser-incision or drilling in this application. From Figure 6, it may be noted that the circularity of the incised holes remained between 0.9 and 1 for CO_2 laser pulse durations below 10 ms and showed no significant change with an increase in laser power. However, the circularity showed a decreasing trend with CO_2 laser power for pulse durations above 50 ms. Similar behaviour can also be seen in Figure 8 and Figure 9 for European Redwood and Beech, respectively. However, a clear indication of the effect of laser power on the circularity of incised holes is evident from Figure 9 which may have been a result of the Beech having a higher density. The decrease in the circularity of CO_2 laser-incised holes with increased laser power in the Beech samples is believed to be because of the increased heat input, resulting in material removal that was likely forced outwards since there was less space in the wood structure for it to go into. The observed effect of laser power on the circularity of CO_2 laser-incised holes was reversed in the Radiata Pine samples, as shown in Figure 7. The circularity of the CO_2 laser-incised holes showed a decreasing trend with laser power for pulse durations below 10 ms which then showed an increasing trend for pulse durations greater than 50 ms. In Southern Yellow Pine, the poor circularity of the CO_2 laser-incised holes, using laser powers from 70 W to 100 W, was observed to relate to abrupt changes which can be attributed to the interaction and transition of earlywood and latewood tissue planes

as the CO_2 laser moves through the wood. This is significant as the earlywood and latewood tissues would have had differing ablation rates due to their difference in densities. That is, the Southern Yellow Pine density would be considerably higher than that of the Southern Yellow Pine earlywood [33]. Similar behaviour of circularity can be seen on the radial face of Radiata Pine (Figure 7) and can be explained by the differing interactions between the CO_2 laser and the earlywood and latewood tissue regions.

3.3 Effect of laser power on the depth of incised hole

Figure 10 presents the variation of depth of CO_2 laser-incised holes with laser power in (a, b) Southern Yellow Pine, (c, d) Radiata Pine, (e, f) European Redwood and (g, h) Beech for different laser pulse durations. The plots shown in Figure 10 (a, c, e, g) illustrate the effects on the radial face and plots Figure 10 (b, d, f, h) illustrate the effects on the tangential face. From Figure 10, an increase in laser power from 70 W to 170 W gave rise to an increase in the depth of the CO_2 laser-incised holes. However, the increase in the depth of laser-incised holes was not monotonic in nature, implying that other factors (earlywood and latewood presence, sequence, orientation, thickness etc) were involved in determining the final depth of CO_2 laser-incised holes, as explained in Figure 5. In Southern Yellow Pine, the variation in depth of CO_2 laser-incised holes with laser power was not significant at lower pulse durations (below 10 ms) although there was an increasing trend above 50 ms on the radial face as shown in Figure 10 (a). The tangential face of Southern Yellow Pine, however, showed no effect following an increase in laser power, which indicated other factors are responsible here. With multiple growth rings in the Southern Yellow Pine, that were relatively evenly spaced compared to the other wood species, it is likely that the CO_2 laser processed as many

earlywood tissue layers as latewood tissue layers. As a direct result of this, it is likely that this phenomenon led to the observed negligible effect on the depth of the CO_2 laser-incisions. A similar behaviour was observed for European Redwood, as shown in Figure 10 (e, f) and, again, is likely since the European Redwood had a very high number of growth rings per centimetre compared to the other species studied (Radiata Pine and Beech). The effect of the increase in CO_2 laser power on the depth of the CO_2 laser-incised holes was evident at all pulse durations in the Radiata Pine and the Beech, as shown in Figure 10 (c, d) and Figure 10 (g, h), respectively. The resulting increase in hole depth with increased CO_2 laser power was due to the increased energy/heat input which subsequently accelerated melting and vaporisation in the laser-material interaction zone. With Radiata Pine and Beech having growth rings that are wider spaced compared to the Southern Yellow Pine and the European Redwood, it is also likely that this would have had a significant impact on the CO_2 laser incision process. For instance, if the CO_2 laser was to pass through a latewood tissue region early in the incision process then the CO_2 laser-incision depth would have been subsequently attenuated (see Figure 5(b)). On the other hand, if the CO_2 laser was to pass through a region of earlywood tissue the CO_2 laser beam would be able to process this less dense wood efficiently, giving rise to a deeper incision due to less attenuation (see Figure 5(a)). The maximum depth measured on the radial faces for Southern Yellow Pine, Radiata Pine, European Redwood and Beech were ~ 26 mm, ~ 30 mm, ~ 34 mm and ~ 26 mm, respectively. The maximum CO_2 laser-incised hole depth measured on the tangential faces of Southern Yellow Pine, Radiata Pine, European Redwood and Beech were ~ 23 mm, ~ 30 mm, ~ 23 mm and ~ 23 mm, respectively. The smallest depths of CO_2 laser-incised holes were measured in Beech and can be explained due to the denser nature of this wood species (*cf*. Table 1) compared to the other wood species studied.

The maximum depth of CO_2 laser-incised hole was measured in Radiata Pine and was due to its low density compared to the other wood species studied. Comparing the radial and tangential faces of Southern Yellow Pine, Radiata Pine, European Redwood and Beech, it should be noted that the maximum depth measured when CO_2 laser-incised on the radial face was greater than that observed on the tangential face, except for the Radiata Pine samples where the difference was not so significant (and density difference between EW and LW is lower). The dominant effect of the tangential face over the radial face in reducing depth of the CO_2 laser-incised holes is believed to relate to the growth ring structure (see Figure 5), due to the number of layers of latewood per unit length which must be overcome by the laser incision process, as shown in Figure 1. Taking Figure 5 into further consideration, the incision depth, d_3, with the CO_2 laser incident on the tangential face (see Figure 5(c)) would typically be smaller than the CO_2 laser-incision depth, d_1, whereby the CO_2 laser-incision would take place in earlywood only (see Figure 5 (a)). For the relatively rare case where the CO_2 laser-incision would take place exclusively in latewood (see Figure 5(b)), the incision depth, d_2, would be smaller than that of d_1 and d_3. During the CO_2 laser-incision process conducted with this work, it should be noted that CO_2 laser-incision within latewood only may have occurred in a minor number of Southern Yellow Pine samples given the growth ring structure to the Southern Yellow Pine. The fourth scenario (see Figure 5(d)), where the earlywood/latewood tissue growth rings are at an angle to the incident CO_2 laser beam, the incision depth, d_4, would be dependent on the angle of the growth rings to the incident CO_2 laser beam and the circularity/non-circularity of the growth rings. This is owed to the fact that this would determine the amount of earlywood and latewood tissues that the CO_2 laser beam would need to pass through in order to make the incision. One can see that the fourth scenario is more akin to a real-life situation as the

growth rings within wood are not usually perfectly circular and it was observed within the samples that the growth rings did tend to have different, non-idealistic orientations.

3.4 Effect of pulse duration on the diameter of incised holes

Figure 11 shows the variation in diameter of the CO_2 laser-incised holes with laser pulse duration in (a, b) Southern Yellow Pine, (c, d) Radiata Pine, (e, f) European Redwood and (g, h) Beech for different CO_2 laser powers. The plots shown in Figure 11 (a, c, e, g) illustrate the effects on incisions into the radial face and plots Figure 11 (b, d, f, h) illustrate the effects on incisions into the tangential face. It is evident from Figure 11 (a-h) that the diameters of the CO_2 laser-incised holes increased with CO_2 laser pulse duration. The increased laser interaction time with all of the wood species led to an increased heat input which in turn increased the CO_2 laser-incised hole diameter. It is to be noted that the evolution of the diameter with CO_2 laser pulse duration showed a non-linear relationship. It also showed a two-stage regime divided according to specific pulse durations. The 1st regime was seen with pulse durations below 10 ms and the 2nd regime was seen with pulse durations above 50 ms. In the first stage (regime 1), the CO_2 laser-incision rate was faster whereby, in the later stage (regime 2), the CO_2 laser-incision rate was much slower. A maximum CO_2 laser-incised hole diameter of ~ 1.3 mm was measured in Radiata Pine whereas the lowest of ~0.7 mm was measured in Beech. The differences observed was likely the result of density variation between the species, as presented in Table 1.

To understand the CO_2 laser-incision behaviour of the different wood species in regime 1, for shorter pulse durations, the data is re-presented in Figure 12 (a-h). As observed from Figure 12 (a-f), the diameter of the CO_2 laser-incised holes increased linearly with the CO_2 laser pulse duration in most cases for Southern Yellow Pine, Radiata Pine and

European Redwood, except in a few cases where there appears to be an anomaly in the trend. The variation of CO_2 laser-incised hole diameter with CO_2 laser pulse duration in Beech (Figure 12 (g, h)) was seen to be non-linear. Although, a linear behaviour for the Beech samples was observed up to a CO_2 laser pulse duration of 5 ms.

To understand the two different regimes (1 and 2), the mechanism of the CO_2 laser incision process must be considered. In a laser incision process, the material removal takes place by ejection from the hole front as shown in Figure 13. In regime 1, the laser-wood interaction leads to material removal by ejection of vaporised species from the hole front. The ejection of vapour species leads to erosion of the hole wall near the surface contributing to an increase in the laser-incised hole diameter. In regime 1, the laser-incised hole depth was smaller as compared to regime 2. So, the available laser power density in regime 1 was more which contributed to the observed faster incision or material removal, leading to the faster increase in laser-incision hole diameter. In regime 2, the power density decreased with depth as well as there being less laser energy available due to the maximum absorption by the hole wall near the surface. The less laser energy available at the hole front in regime 2 led to the observed slowing down of the laser-incision rate or material removal rate.

3.5 Effect of pulse duration on the circularity of incised holes

Hole circularity was observed to be optimized at low CO_2 laser pulse durations, and decreased with increasing CO_2 laser pulse duration in Southern Yellow Pine, Radiata Pine, European Redwood and Beech, as shown in Figure 14 to Figure 17, respectively. Circularity close to unity is desirable for acceptance in commercially manufactured timber products. The increased laser-wood interaction time from increased CO_2 laser pulse duration, along with the differences between densities of earlywood and latewood

regions, were responsible for the circularity moving away from unity. The anomalous data points in the plots were also due to the differences in densities of earlywood and latewood, an aspect which should always be accounted for when processing wood materials. It is important to mention here that the increased density of the latewood led to an increased absorption of the CO_2 laser radiation by the cell tissues whereas earlywood tissues cells led to lesser absorption and likely more reflection to other regions.

3.6 Effect of pulse duration on the depth of incised holes

Figure 18 shows the variation in depth of the CO_2 laser-incised holes with CO_2 laser pulse duration in (a, b) Southern Yellow Pine, (c, d) Radiata Pine, (e, f) European Redwood and (g, h) Beech at different CO_2 laser powers. The plots shown in Figure 18 (a, c, e, g) are for the radial faces and plots Figure 18 (b, d, f, h) are for the tangential faces. The depth of the CO_2 laser-incised holes increased with CO_2 laser pulse duration. From Figure 18, it is evident that the CO_2 laser-incision rate was highest at shorter CO_2 laser pulse durations, slowing down at longer CO_2 laser pulse durations. This was identified as two different regimes depending on the CO_2 laser pulse durations. In the lower CO_2 laser pulse duration regime 1 (onset of incision), the CO_2 laser-incision speed was rapid which saturated in the later stage. The CO_2 laser power density was a maximum on the surface of each of the samples and just below the surface of the samples within the depth of focus of the laser beam. The CO_2 laser power density then decreased with depth as shown in Figure 19. The diverging CO_2 laser beam had an increasing beam diameter which also contributed to the lowering of the CO_2 laser power density. The decreasing CO_2 laser power density with depth of the CO_2 laser-incised

holes was responsible for the saturation in the laser-incision drilling rate for the CO_2 laser-incision process.

Figure 20 shows the effect of CO_2 laser pulse duration on the depth of the CO_2 laser-incised holes for short pulse durations (up to 10 ms) for (a, b) Southern Yellow Pine, (c, d) Radiata Pine, (e, f) European Redwood and (g, h) Beech. The plots shown in Figure 20 (a, c, e, g) illustrate the effects on the radial face and plots Figure 20 (b, d, f, h) illustrate the effects on the tangential face. Rapid CO_2 laser-incision was evident in lower pulse durations up to 10 ms. This is attributed to the maximum available CO_2 laser power density up to 10 ms pulse duration range as shown in Figure 19.

3.7 Effect of focal length of lens on the characteristics of incised holes

The focal length of the lens during the CO_2 laser-incision process also had a significant impact on the CO_2 laser-incision efficiency. Figure 21 (a-d) shows the effect of 127 mm and 190 mm focal lengths on the diameter and depth of the laser-incised holes in the radial and tangential faces of Southern Yellow Pine. This is likely due to the influence of the wood structure when laser-incising the radial face. For example, when laser-incising into regions of denser latewood rather than earlywood. The theoretical values of the CO_2 laser beam diameter and depth of focus were calculated using Equation (4) and Equation (5) for the two different focal lengths used and the values are presented in Table 3.

It is evident from Table 3 that with the increase in the focal length of the lens, the diameter of the CO_2 laser beam at the focal plane increased. From Figure 21 (a, b), the CO_2 laser-incised hole diameter increased with an increase in the focal length of the lens. This was due to the increase in the theoretical beam diameter with increase in the focal length of lens. However, the measured CO_2 laser-incised hole diameter was much

higher than the theoretical CO_2 laser beam diameter at the focal plane. Similarly, a higher theoretical depth of focus was evident with an increase in the focal length of the lens as presented in Table 3. The increase in depth of focus was more than double, with a change in focal length from 127 mm to 190 mm of the lens. The increase in depth of focus also resulted in less taper of the CO_2 laser-incised holes and helped to maintain a uniform CO_2 laser power density to a certain depth. It was expected that the depth of the CO_2 laser-incised hole should be higher for longer focal lengths. From Figure 21 (c, d), it can be seen that the radial face showed no significant difference in the depth of the CO_2 laser-incised holes with 127 mm and 190 mm focal lengths. The presence of the dense latewood along the path of the laser radiation, during the laser-incision process, was likely the reason behind this observed anomaly.

3.8 Effect of focal length on circularity of incised holes

Figure 22 shows the effect of focal length of lens on the circularity of CO_2 laser-incised holes on the radial and tangential faces of the wood samples. It is evident that the focal length of the lens had a strong effect on the circularity of the CO_2 laser-incised holes. The differences observed in the circularity of the CO_2 laser-incised holes with 127 mm and 190 mm focal lengths was less in the short pulse duration regime compared to larger pulse durations. The circularity of the CO_2 laser-incised holes with a 127 mm focal length gradually decreased with increasing pulse duration as shown in Figure 22. However, with a 190 mm focal length the circularity of the CO_2 laser-incised holes showed no significant change and remained close to unity at all pulse durations, as evidenced in Figure 22. The improved circularity with longer focal length is likely due to the larger focal spot size, lower CO_2 laser power density and the longer depth of focus which maintained a constant CO_2 laser power to a certain depth.

3.9 Effect of focal point positioning on the characteristics of incised holes

Focal point positioning of the CO_2 laser beam can control the quality and process efficiency during laser material processing. To better understand the focal point positioning effect on CO_2 laser-incision efficiency, z ± 5 mm variation in distance from the focal plane was kept as shown in Figure 23.

Figure 24 shows the effect of the focal point positioning on the diameter and depth of the CO_2 laser-incised holes in Southern Yellow Pine, incised with a CO_2 laser power of 170 W. The influence of the focal point positioning on the CO_2 laser-incision hole diameters and hole depths is shown in Figure 24. With the CO_2 laser beam focused 5 mm away from the wood surface (z = + 5 mm), the CO_2 laser-incised hole diameter was a maximum value since a diverging laser beam with higher beam diameter was incident on the surface of the sample. Comparing the laser power densities with respect to the focal point positions, it can be observed that the diameter of the incised hole is the smallest for a laser power density of 4.81×10^5 W/cm^2 and the largest hole diameter was measured for the sample incised with a laser power of 5.6×10^4 W/cm^2. The observed difference is due to the difference in laser beam diameters on the surface of the wood in both the cases increase rather than the output laser power. However, the diameter of the laser incised hole is higher in the case where the laser beam was focused away from the wood surface (z = + 5 mm) than when the laser beam focussed below the wood surface (z = - 5 mm). It is believed that the converging laser beam is responsible for the smaller hole diameter. On the other hand, the depth of CO_2 laser-incised hole was maximum when the focal point is positioned 5 mm below the surface of the sample (z = - 5 mm) which can be attributed to the converging nature of the CO_2 laser beam irradiating the surface of the sample. However, the difference in depth of

incised holes between the samples with z = 0 mm and z = -5 mm is not significant. Nevertheless, the laser power density is lower in z = -5 mm than z = 0 mm. From Figure 24 (c, d), it may be noted that the lowest depth of the incised hole was measure for the sample incised with the focal point positioned away from the surface of the wood which is attributed to the lower laser power density and diverging nature of laser beam. It is, therefore, advantageous to focus the laser beam below the surface of the sample to achieve higher depth of incision and a moderate increase in diameter of the CO_2 laser-incised holes.

3.10 Hole shape and quality analysis

Figure 25 shows the CO_2 laser-incised holes when viewed from above on the radial face of (a) Southern Yellow Pine (b) Radiata Pine, (c) European Redwood and (d) Beech with a CO_2 laser power of 170 W and a pulse duration of 1 ms (a-d) and 80 ms (e-h). From Figure 25, it can be seen that the shape of the CO_2 laser-incised holes were near circular when incised with a pulse duration of 1 ms. With pulse durations of 80 ms, the CO_2 laser-incised holes gave rise to poor circularity due to increased laser–wood interaction time as evident from Figure 25 (e-h). The holes incised with a lower CO_2 laser pulse duration (1 ms) also showed less charring, whereas the holes incised with a longer CO_2 laser pulse duration (80 ms) showed significant charring. It should be noted that all the experiments were conducted without any process gas. Use of nitrogen gas is normally used to reduce charring by providing a cooler environment and to reduce the level of oxygen by implanting an inert gas in laser cutting processes [34]. From Figure 25 (a-d), it may be noted that the colour change on the surface of the incised holes is yellow which changes to a darker colour as shown in Figure 25 (e-h). The colour change in the wood samples following CO_2 laser processing has been previously

reported [35, 36] and is believed to be due to the oxidative degradation of hemicellulose, cellulose and lignin. The yellow colour change in the CO_2 laser modified wood, with short pulse durations, is due to the degradation of lignin [37]. With an increase in pulse duration up to 80 ms, the darkening of the CO_2 laser-incised holes can be observed due to degradation of the hemicellulose [35]. The influence of charring and incision diameter on uptakes of preservative liquids during treatment requires further testing, and would likely be an important factor which could govern the suitability and application of laser incision technology in wood treatments and related manufacturing processes.

Observing the cross-sections of the CO_2 laser-incised holes also showed significantly less charring with a shorter pulse duration (1 ms) compared to a longer pulse duration (80 ms), as shown in Figure 26. A reduction in charring offers an aesthetic benefit for product development using laser incision systems. It should also be noted that the presence of latewood tissue impacted on the CO_2 laser-incised hole depth, as can be seen in Figure 26 (a). The denser latewood absorbed the maximum laser energy and reflected less of the laser radiation, leading to a reduction in laser-incision depth. Extension of charring may be seen in Figure 26 (h) which could be the result of interaction of the CO_2 laser radiation with rays aligned perpendicular to incident laser. The cross-section presented in Figure 26 (d) shows darkening of the cell structure. Significant darkening in the CO_2 laser-incised hole cross-sections of Southern Yellow Pine, Radiata Pine, European Redwood and Beech was observed and is shown in Figure 6 (e-h). The discolouration in Beech (Figure 26 (h)) was highest compared to the other wood species studies and is likely related to the chemical structure of the Beech wood. The spreading of discolouration lines at some points as marked by arrows along the

CO_2 laser-incised hole depth implies severe structural degradation at the marked places along the depth of the CO_2 laser-incised hole.

Figure 27 illustrates the calculated peak surface temperatures in (a) Southern Yellow Pine, (b) Radiata Pine, (c) European Redwood and (d) Beech during CO_2 laser-incision at different CO_2 laser powers and CO_2 laser pulse durations. It is evident from Figure 27 that the peak surface temperature calculated was maximum in the Radiata Pine (8467 °C) and minimum in the Beech (5376 °C). The surface temperature reached up to 8000°C on both Southern Yellow Pine and Radiata Pine whereas the peak surface temperature of nearly 6470°C was calculated for the European Redwood. A peak surface temperature of ~5376°C was calculated for the Beech samples. It is likely that the wood density and moisture content had a role in controlling the peak surface temperature. The higher surface temperatures calculated in the Southern Yellow Pine and the Radiata Pine can be attributed to their lower moisture content and density. The lowest surface temperature calculated was for the Beech samples, the wood species with the highest density and the highest moisture content. The peak rise in temperature during the CO_2 laser-incision process can also be attributed to the absence of process gas which tends to reduce the temperature during the laser-incision process. It has been reported that during CO_2 laser cutting of wood the surface temperature can rise to temperatures around 4750 °C [38]. The surface temperatures observed are likely to have caused the decomposition of the wood structural materials, as hemicelluloses generally decompose at 170–260 °C, cellulose at 240–350 °C and lignin at 280–550 °C [22], all well below the calculated temperatures.

Figure 28 shows the finite element simulation of temperature rise on the surface of Southern Yellow Pine during laser incision at (a, b) a laser power of 70 W and a pulse

duration of 1 ms and (c, d) a laser power of 170 W and a pulse duration of 80 ms. The temperature distribution in the wood surface is shown in different colours. From Figure 28 (a, b), it can be seen that the temperature rise is maximum at the centre and decreases towards the edge of the hole. The maximum temperature rise was calculated to be 546 °C (819 K) at a laser power of 70 W and a pulse duration of 1 ms. With an increase in laser power to 170 W and a pulse duration to 80 ms, the peak rise in temperature increased to 9957 °C (10230 K). The laser power and pulse duration have a significant effect on increasing the temperature on the surface of the wood as the heat flux into the wood surface increases with laser power density. One of the possible reasons for the increase in temperature on the wood surface is also related to the absence of assisting gas supply in the present study which is believed to reduce the temperature. Conduction and convection losses are very low due to the fact that the thermal conductivity of wood is low and the absence of any assisting gas, respectively. The calculated temperature in the finite element analysis may be corroborated to the analytical values presented in the previous section.

Figure 29 shows the scanning electron micrographs of un-incised (a) Southern Yellow Pine, (b) Radiata Pine, and (c) Beech. Presence of bordered pits (marked by arrows) in the tracheids of the Southern Yellow Pine and the Radiata Pine can be seen in Figure 29 (a, b). These pits control the flow between the tracheid elements in softwoods. Vessels are visible in Figure 29 (c), and dominate the flow of liquids in hardwood timbers. Pitting between vessel cells (marked Pv) is simple, and flow is predominantly aligned with the vessel cells. Pits between vessels and ray cells (Pv-r) and between vessels and tracheids (Pv-t) have smaller apertures, and play only a secondary role in flow. The ray cells, also seen in Figure 29 (a, c) are responsible for relatively minor

fluid flow radially within the tree trunk and may contribute to fluid flow to a small extent during preservative treatments.

Figure 30 shows the scanning electron micrographs of CO_2 laser-incised regions in (a) Radiata Pine, (b) Southern Yellow Pine, and (c) Beech with a CO_2 laser power of 170 W and a CO_2 laser pulse duration of 80 ms. The CO_2 laser-incision process induced removal and degradation of the wood tissue, and induced localised associated structural changes, as seen in Figure 30. Presence of debris may be observed in the structure of Southern Yellow Pine and Radiata Pine which was due to the sanding operation used to expose the cross-section of the CO_2 laser-incised holes. Formation of fine textured pores on the remaining cell wall edges (indicated by dashed circles in Figure 30 (a) and Figure 30 (b)), as well as separation of the cells at the middle lamella (Figure 30 (b)), were evident. Some pores were observed in the inner face of the cell wall near the CO_2 laser incision, as if gas or plasma were erupting from beneath the surface (Figure 30 (b), denoted by hollow arrows). The formation of these pores is thought to be a result of the peak rise in temperature from the incident CO_2 laser beam on the sample surface. There may be two possibilities giving rise to these porous structures on the wood cell wall at the perimeter of the incision hole. Firstly, the peak rise in temperature during CO_2 laser-incision may have resulted in a cell wall explosion due to increased vapour pressure of trapped water evaporating from within the cell wall. Secondly, the formed porous structure at the CO_2 laser-incision point may be due to charring of wood structure, degradation of lignin and cellulose, and differences in the rate of evaporation or plasma-generation from the three constituent wood wall polymers as reported by others [21- 23, 35]. From Figure 30 (c), some re-deposition took place on the cell walls, which are not completely porous. This implies some melting of the cell wall, with the

melt consisting of lignin and polysaccharides. Similar structural modification has been observed in laser cutting of woods [32, 39]. The increased deposition on the cell wall and charring may also be related to the non-use of the process gas in the present work. The use of non-reactive process gas during laser cutting of woods is preferred as it helps to reduce charring [40]. Laser cutting with a CO_2 laser was reported to form a layer of char on the wood surface due to generation of significant amount of heat [39, 40]. Melting and carbonisation of cellulose following laser ablation was reported for UV and IR radiations [21]. It should also be noted that CO_2 laser also causes thermal modification in wood [35]. The laser induced damage was mostly localised on the wall and had no significant effect on nearby pits which are one of the main influences on permeability. Further laboratory tests are needed to understand the complete effect of CO_2 laser-incising on permeability of these incised structures. The deposition of carbonaceous products in wood following laser irradiation was found to be laser induced graphene (LIG) in some reported works [41-43]. The chemical composition of wood has a strong influence of the deposition of these products as higher lignin contents in wood tend to lead to easy carbonisation and formation of LIG [42]. Moreover, the formation of LIG occurs at a low laser power (1.6 to 8.6 W) with a shorter pulse duration under an inert atmosphere [41, 43]. However, comparatively much higher laser powers, with longer pulse durations, without any gas supply was used in the present study. The structural modifications in regime 1 and regime 2 were found to be similar in the laser-incised holes. The temperature rise in the wood is in excess of 500 °C as shown in Figure 27 and Figure 28 which is significant in altering the structure of the wood [22].

4. Conclusions

This work investigated some of the main factors influencing quality of CO_2 laser-incisions in wood. It was found that both laser power and pulse duration influenced the CO_2 laser-incised hole size and shape. Laser parameters such as focal length of lens and focal point position in the sample were also found to have an effect on CO_2 laser-incised hole characteristics. This work has shown the importance of the need to consider earlywood and latewood interactions with the CO_2 laser during the incision process, given the different material characteristics (especially density) of the earlywood and latewood tissues. Further consideration has also been given within this work to show the importance of considering the impact of wood orientation during the CO_2 laser-incision process. The incisions into radial, tangential or intermediate faces of the timber alter the growth ring alignment, number of rings traversed, and incision depth. The presence of two distinct CO_2 laser-incision mechanisms were also found which showed faster incision rate in the onset of the laser incision process (regime 1) and slowing down in the later stage (regime 2). The following conclusions may be drawn:

1. A CO_2 laser was found to be successful in laser-incising Southern Yellow Pine, Radiata Pine, European Redwood and Beech; wood species with densities ranging from 400 to 730 kg/m^3, to a desired hole depth.
2. Increase in the depth and diameter of CO_2 laser-incised holes were observed with an increase in CO_2 laser power. However, the influence of CO_2 laser power on holes varied with the wood density, with higher density reducing incision depth.
3. Increasing CO_2 laser pulse duration increased both the depth and diameter of the CO_2 laser-incised holes, although circularity of the incisions was decreased with increasing CO_2 laser pulse duration. Desired hole depths can be achieved by using appropriate pulse durations.

4. Presence of two distinct incision mechanisms was found which showed faster incision rate in the onset of incision process (regime 1) with slowing down in the later stage (regime 2).
5. Increased CO_2 laser pulse duration also led to increased charring.
6. With a lens of longer focal length, both the depth and diameter of CO_2 laser-incised holes increased.
7. The circularity of incised holes was close to unity for a focal length of 190 mm than 127 mm.
8. Positioning the focal point below the surface of sample resulted in an increase in the depth of CO_2 laser-incised holes.
9. Wood anatomy had a major influence on the depth of CO_2 laser-incising when incised at the same CO_2 laser power. It was evident that denser wood reduced the rate of incision, which was seen between species and also within growth rings, where denser latewood reduced the CO_2 laser incision depth.
10. Localised CO_2 laser induced modification of wood structure was evident in the CO_2 laser-incised holes. Deposition of residue and melting of the wood structure were observed following CO_2 laser-incision, although no evidence of sealing or closure of lumena or pits were observed. This suggests that such CO_2 laser-incision techniques could positively impact upon the permeability of wood for preservative treatments.

Acknowledgement

Authors would like to thank Mr. Daniel Beresford and Mr. Steve Allitt for their help and support while carrying out the project.

Funding: This work was supported by Innovate UK (LASERCURE: 103545).

References

[1] Eaton R.A., Hale M.D.C., Wood: Decay, Pests and Protection, first ed., Chapman and Hall, London, 1993.
[2] Reinprecht L., Wood Deterioration, Protection and Maintenance, first ed., John Wiley & Sons, West Sussex, 2016.
[3] Perrin P.W., Review of incising and its effects on strength and preservative treatment of wood, Forest. Prod. J. 28 (2) (1978) 27–33.
[4] Basics of Pressure Treatment of Wood, Oklahoma Cooperative Extension Service, OSU Extension Fact Sheets, http://www.factsheets.okstate.edu/documents/nrem-5047-basics-of-pressu re-treatment-of-wood/, 2016. (accessed October 2016).
[5] Wilkinson J.G., Industrial Timber Preservation, first ed., Associated Business Press, London, 1979.
[6] Comstock G.L., Côté Jr. W.A., Factors affecting permeability and pit aspiration in coniferous wood, Wood. Sci. Technol. 2 (4) (1968) 279–291.
[7] Dubey A.K., Yadav V ., Laser beam machining—A review, Int. J. Mach. Tool Manu. 48 (6) (2008) 609–628.
[8] Wang H., Lin H., Wang C., Zheng L., Hu X., Laser drilling of structural ceramics—A review, J. Eur. Ceram. Soc. 37 (2017) 1157–1173.
[9] Gautam G.D., Pandey A.K., Pulsed Nd: YAG laser beam drilling: A review, Opt. Laser. Technol. 100 (2018) 183–215.
[10] Dahotre N.B., Harimkar S.P., Laser Fabrication and Machining of Materials, first ed., Springer, Boston, 2008.
[11] Zhou B.H., Mahdavian S., Experimental and theoretical analyses of cutting nonmetallic materials by low power CO2-laser, J. Mater. Process. Technol. 146 (2) (2004) 188–192.
[12] Leone C., Lopresto V ., De Iorio I., Wood engraving by Q-switched diode-pumped frequencydoubled Nd: YAG green laser, Opt. Laser. Eng. 47 (1) (2009) 161–168.
[13] B.H. Klimt, State of the art in laser marking and engraving, Proc. SPIE 0744, Lasers in motion for industrial applications (1 January 1987).
[14] Kamke F.A., Peralta P.N., Laser incising for lumber drying, Forest. Prod. J. 40 (4) (1991) 48–54.
[15] S.D. Cichowlaz, Wood preservation & wood products treatment pest control study guide, Nevada state department of agriculture, 10 (2004/2005), 1–59.
[16] Perré P., Karimi A., Fluid migration in two species of beech (Fagus silvatica and Fagus orientalis): a percolation model able to account for macroscopic measurements and anatomical observations, Maderas. Cienc. Tecnol. 4 (1) (2002) 50–68.
[17] Hansmann C., Gindl W., Wimmer R., Teischinger A., Permeability of wood - A review, Wood. Res. 47 (2002) 1–16.
[18] Kakaras A., Voulgaridis E.V ., Effect of ponding, steaming and drill perforation on preservative treatment of fir wood (Abies cephallonica L.) with CCB, Eur. J. Wood. Wood. Prod. 50 (1992) 275–279.

[19] Morrell J.J., Gupta R., Winandy J.E., Ryanto D.S., Effects of incising and preservative treatment on the shear strength of 2 inch lumber, Wood. Fiber. Sci. 30 (4) (1998) 374–382.
[20] Dahlan M.J., Improving the quality of treated timber by incising, Fifth Conference on Forestry and Forest Product Research (CFFPR), Forest Research Institute Malaysia, Kepong, 1999, pp. 1– 10.
[21] Panzner M., Wiedemann G., Henneberg K., Fischer R., Wittke T., Dietsch R., Experimental investigation of the laser ablation process on wood surfaces, Appl. Surf. Sci. 127 (129) (1998) 787–792.
[22] Wang Y ., Ando K., Hattori N., Changes in the anatomy of surface and liquid uptake of wood after laser incising, Wood. Sci. Technol. 47 (2013) 447–455.
[23] Barcikowski S., Koch G., Odermatt J., Characterisation and modification of the heat affected zone during laser material processing of wood and wood composites, Holz. Roh. Werkst. 64 (2006) 94–103.
[24] Le Harzic R., Huot N., Audouard E., Jonin C., Laporte P., Valette S., Fraczkiewicz A., Fortunier R., Comparison of heat-affected zones due to nanosecond and femtosecond laser pulses using transmission electronic microscopy, Appl. Phys. Lett. 80 (21) (2002) 3886–3888.
[25] Kortsalioudakis N., Petrakis P., Moustaizis S., Voulgaridis E., Adamopoulos S., Karastergiou S., Passialis C., An application of a laser drilling technique to fir and spruce wood specimens to improve their permeability, Innovation in Woodworking Industry and Engineering Design, ISSN 2367–6663, 2015, pp. 5–13.
[26] Islam M.N., Ando K., Yamauchi H., Kobayashi Y ., Hattori N., Comparative study between full cell and passive impregnation method of wood preservation for laser incised Douglas-fir lumber, Wood. Sci. Technol. 42 (4) (2008) 343–350.
[27] Hattori N., Ando K., Kitayama S., Nakamura Y ., Laser incising of wood: Impregnation of columns with water-soluble dye, Mokuzai Gakkai-Shi 40 (12) (1994) 1381–1388.
[28] Islam M.N., Ando K., Yamauchi H., Hattori N., Effects of species and moisture content on penetration of liquid in laser incised lumber by the passive impregnation method, Eur. J. Wood. Wood. Prod. 67 (2) (2009) 129–133.
[29] Hattori N., Ida A., Kitayama S., Noguchi M., Incising wood with a 500 watt carbon-dioxide laser, Mokuzai Gakkai-Shi 37 (8) (1991) 766–768.
[30] Naderi N., Legacey S., Chin S.L., Preliminary investigations of ultrafast intense laser wood processing, For. Prod. J. 49 (1999) 72–76.
[31] W.P. Goss, R.G. Miller, Thermal properties of wood and wood products, Thermal performance of the exterior envelopes of buildings, Atlanta, GA, 1992, pp. 193–203.
[32] Kannatey-Asibu E. Jr., Principles of Laser Materials Processing, first ed., Wiley, New Jersey, 2009.
[33] Yusoff N., Rizal Ismail S., Mamat A., Ahmad-Yazid A., Selected Malaysian wood CO2-laser cutting parameters and cut quality, Am. J. Appl. Sci. 5 (8) (2008) 990–996.
[34] Cramer S., Kretschmann D., Lakes R., Schmidt T., Earlywood and latewood elastic properties of loblolly pine, Holzforschung 59 (2005) 531–538.
[35] Hattori N., Matano T., Okamoto H., Okamura K., Microscopic observations of the solid products deposited on the edge of paper by CO2 laser cutting, Mokuzai Gakkai-Shi 34 (1988) 417–422. [36] Kubovsky I., Kacík F., Colour and

chemical changes of the lime wood surface due to CO2 laser thermal modification, Appl. Surf. Sci. 321 (2014) 261–267.
[37] Kacík F., Kubovsky I., Chemical changes of beech wood due to CO2 laser irradiation, J. Photochem. Photobiol. A 222 (2011) 105–110.
[38] Müller U., Rätzsch M., Schwanninger M., Steiner M., Zöbl H., Yellowing and IR-changes of spruce wood as result of UV-irradiation, J. Photochem. Photobiol. B 69 (2003) 97–105.
[39] Li L., Mazumder J., A study of the mechanism of laser cutting of wood, Forest. Prod. J. 41 (10) (1991) 53–59.
[40] Naderi N., Legacéy S., Chin S.L., Preliminary investigations of ultrafast intense laser wood processing, Forest. Prod. J. 49 (6) (1999) 72–76.
[41] Barnekov V .G., McMillin C.W., Huber H.A., Factors influencing laser cutting of wood, Forest. Prod. J. 36 (1) (1986) 55–58.
[42] Ye R., Chyan Y ., Zhang J., Li Y ., Han X., Kittrell C., Tour J.M., Laser-induced graphene formation on wood, Adv. Mater. 29 (2017) 1702211–1702217.
[43] Chyan Y., Ye R., Li Y., Singh S.P., Arnusch C.J., Tour J.M., Laser-induced graphene by multiple lasing: toward electronics on cloth, paper, and food, ACS Nano. 12 (2018) 2176–2183.
[44] Mahmood F., Zhang C., Xie Y ., Stalla D., Lin J., Wan C., Transforming lignin into porous graphene via direct laser writing for solid-state supercapacitors, RSC Adv. 9 (2019) 22713– 22720.

List of Figures

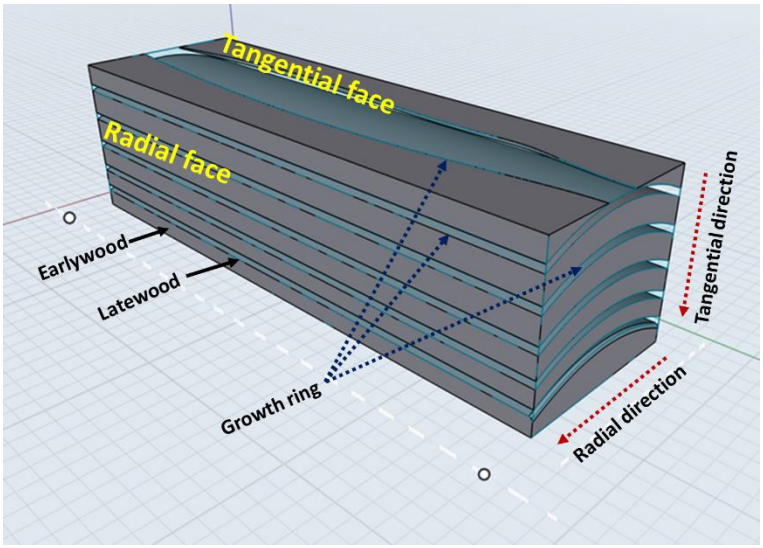

Figure 1 Schematic representation of wood block showing gross anatomy and faces.

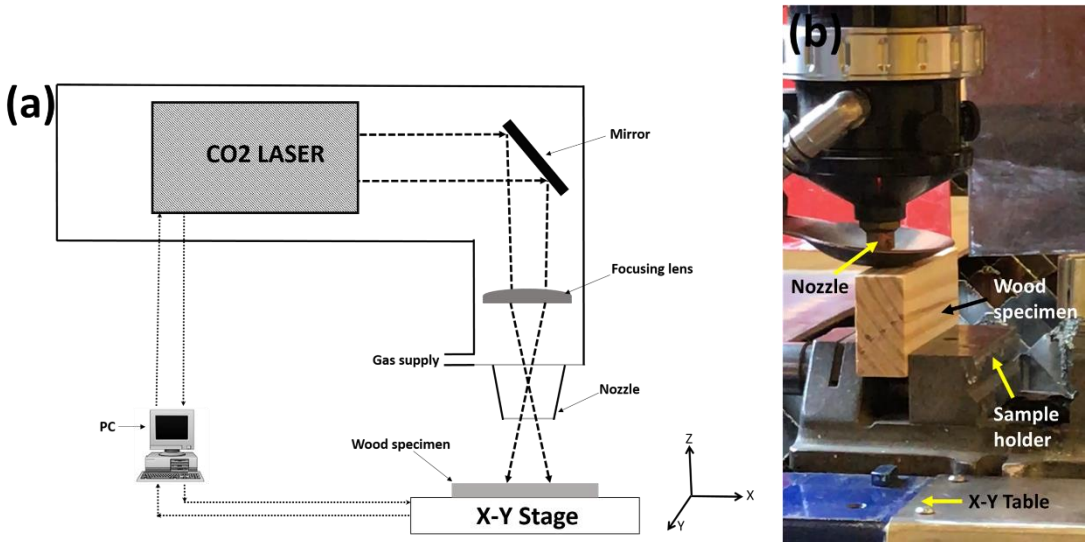

Figure 2 (a) Schematic representation of laser incision set-up and (b) laser incision experimental set-up used in the present study.

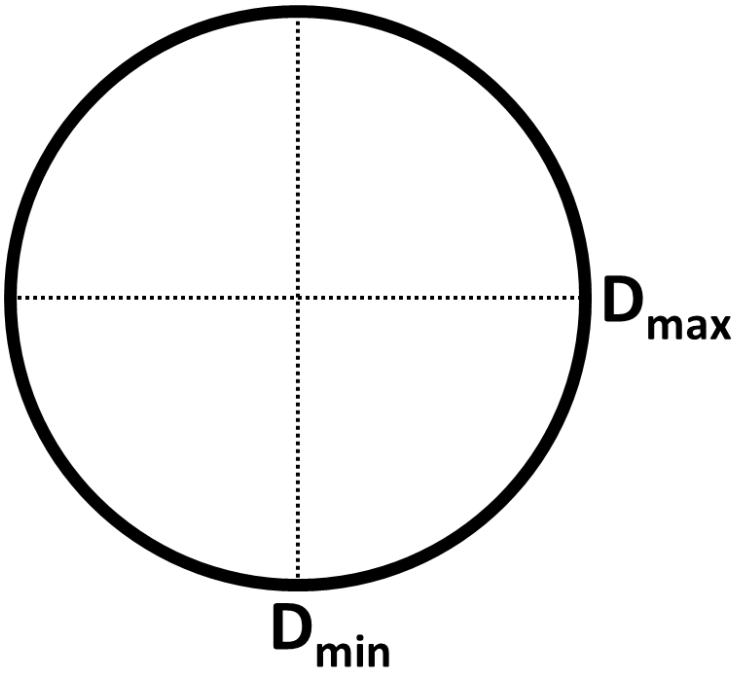

Figure 3 Schematic representation of incised hole diameters used for the calculation of circularity.

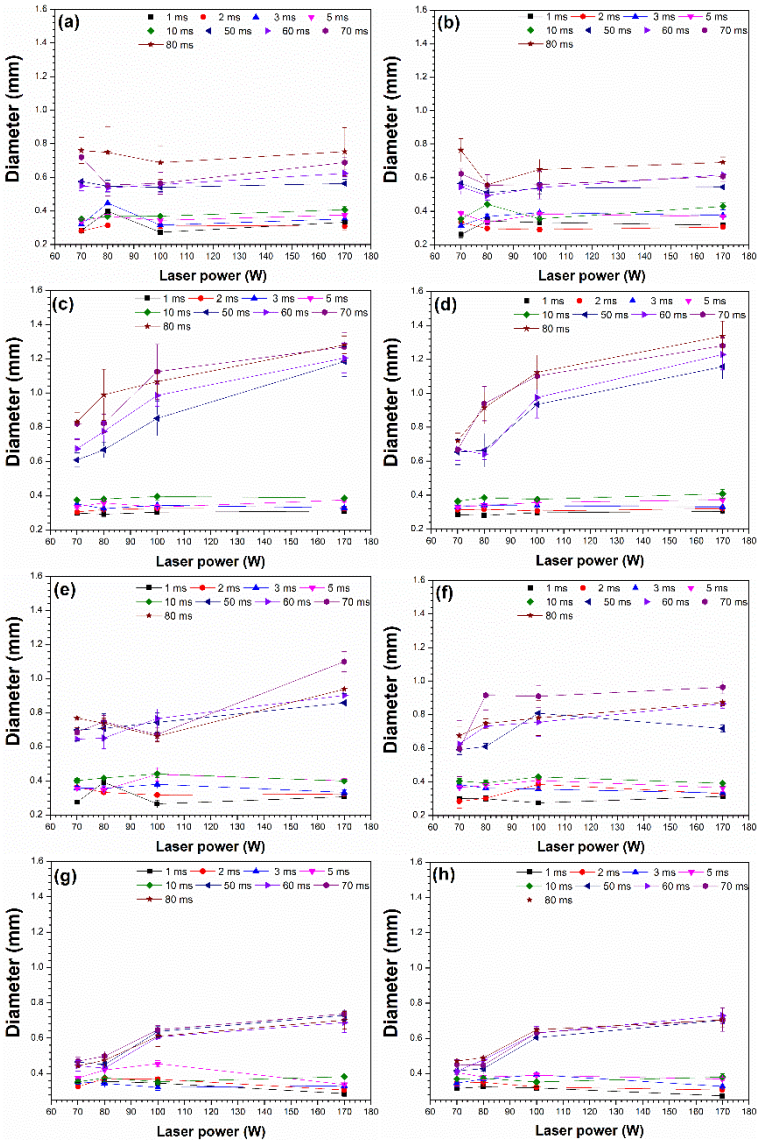

Figure 4 Effects of applied laser power on the diameter of the laser incised holes in (a, b) Southern Yellow Pine, (c, d) Radiata Pine, (e, f) European Redwood and (g, h) Beech. (a, c, e and g represents the radial face and b, d, f and h represents the tangential face).

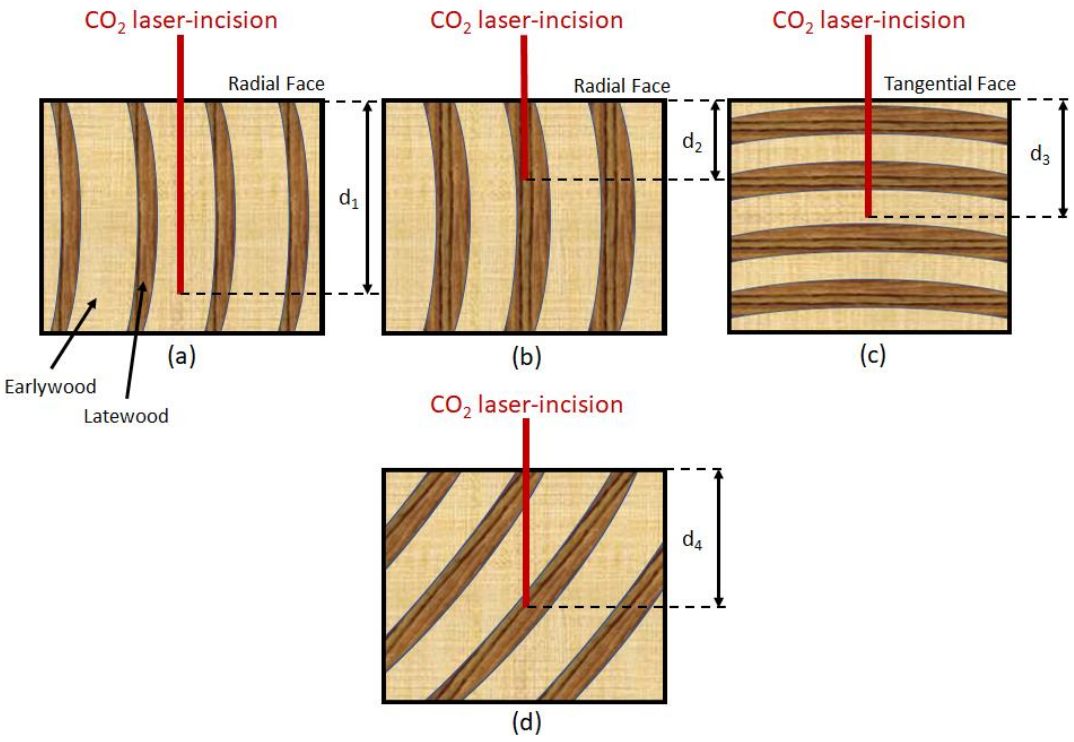

Figure 5 Schematic diagrams of CO_2 laser-incision strategies with CO_2 laser interaction with earlywood and latewood tissues in the structure of wood.

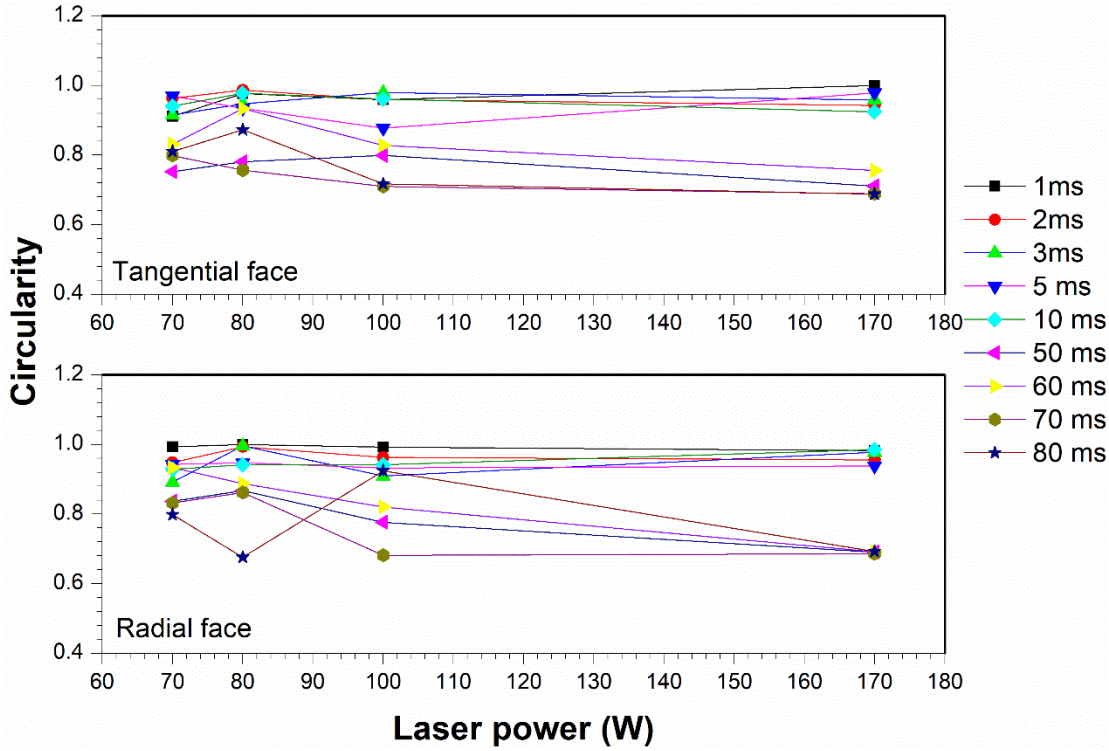

Figure 6 Effect of applied laser power on the circularity of laser incised holes in Southern Yellow Pine.

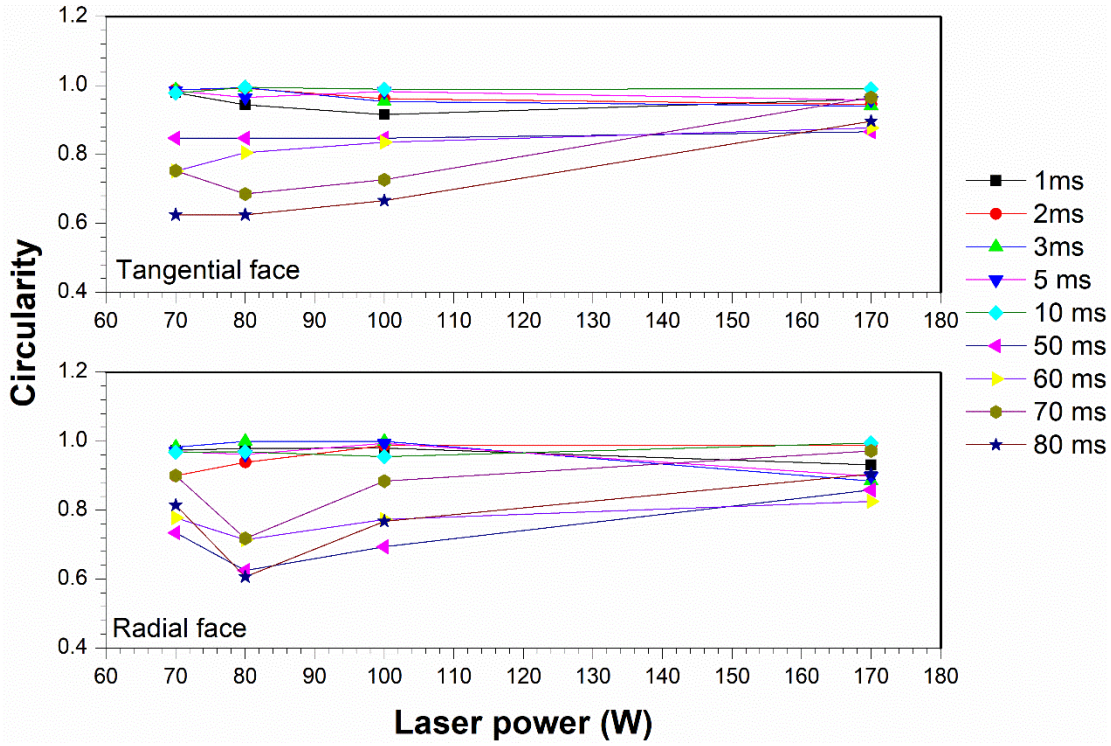

Figure 7 Effect of applied laser power on the circularity of laser incised holes in Radiata Pine.

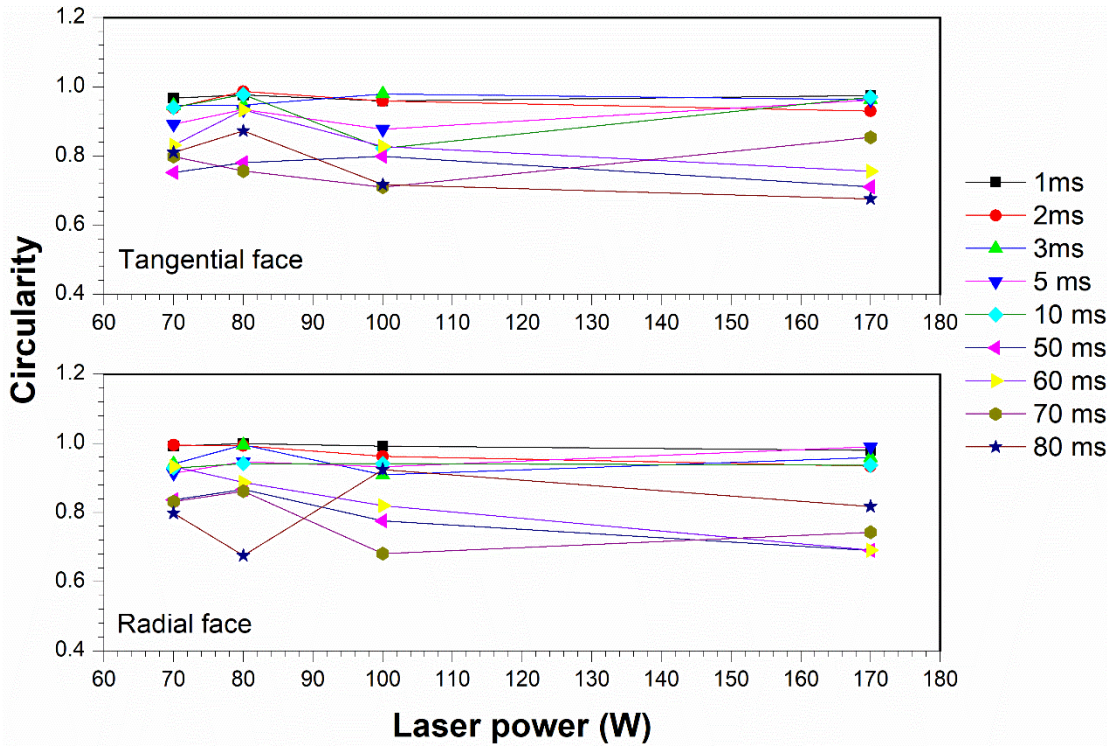

Figure 8 Effect of applied laser power on the circularity of laser incised holes in European Redwood.

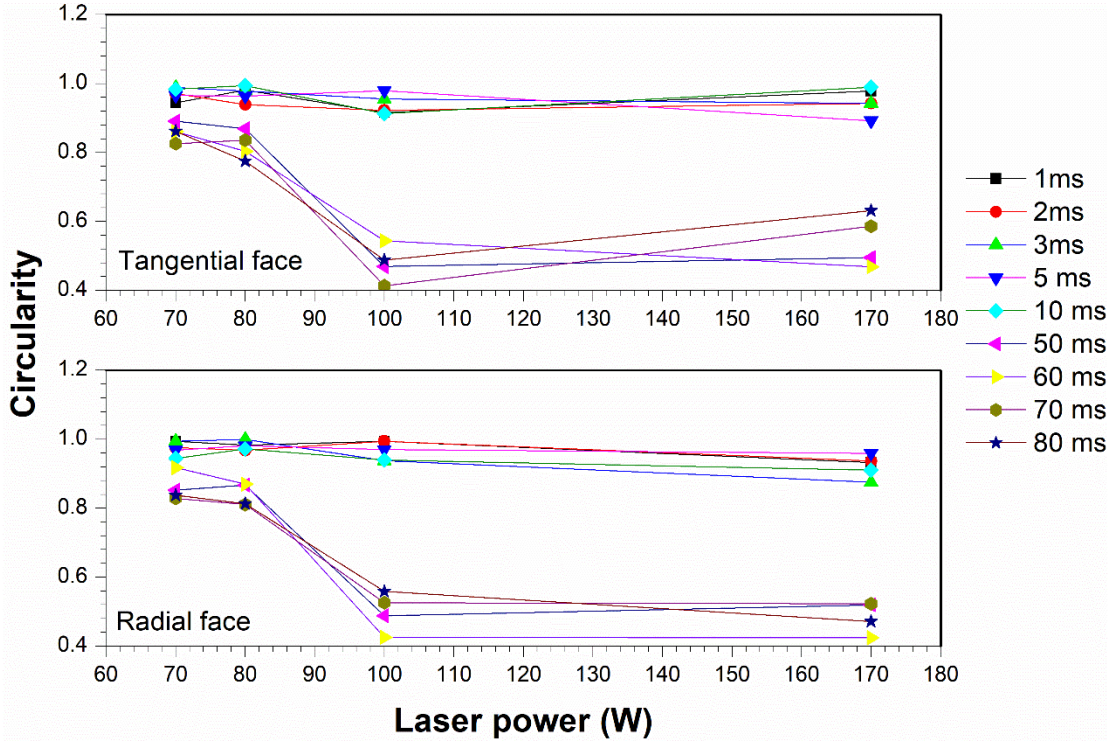

Figure 9 Effect of applied laser power on the circularity of laser incised holes in Beech.

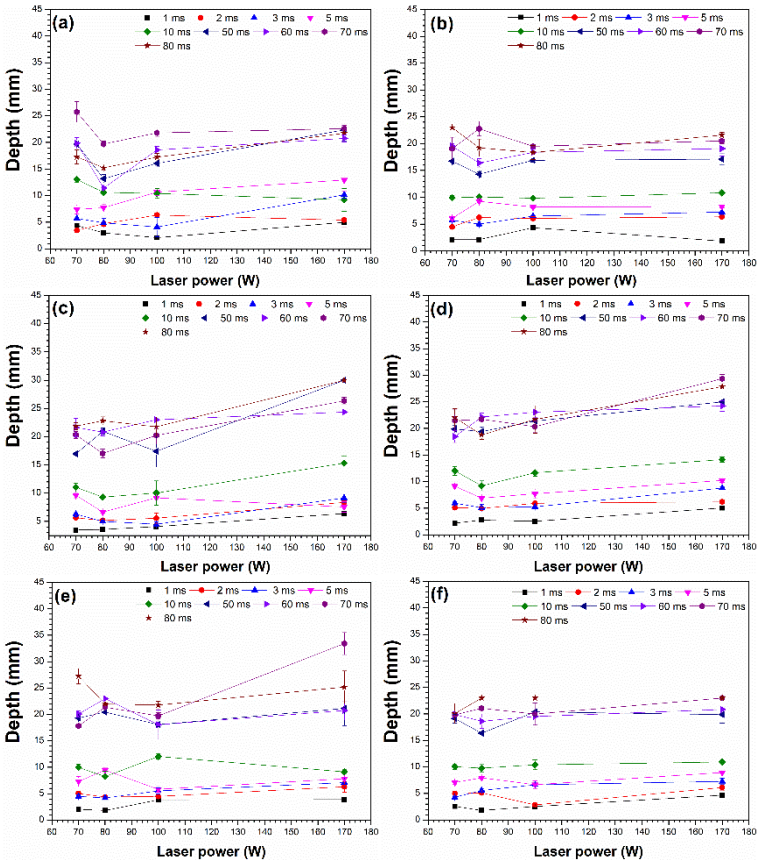

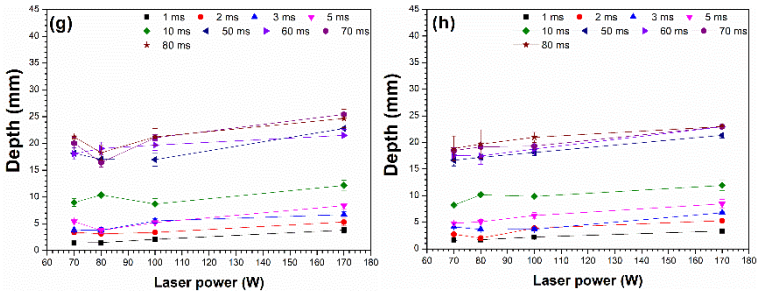

Figure 10 Effect of applied laser power on the depth of the laser incised holes in (a, b) Southern Yellow Pine, (c, d) Radiata Pine, (e, f) European Redwood and (g, h) Beech. a, c, e and g represents the radial face and b, d, f and h represents the tangential face.

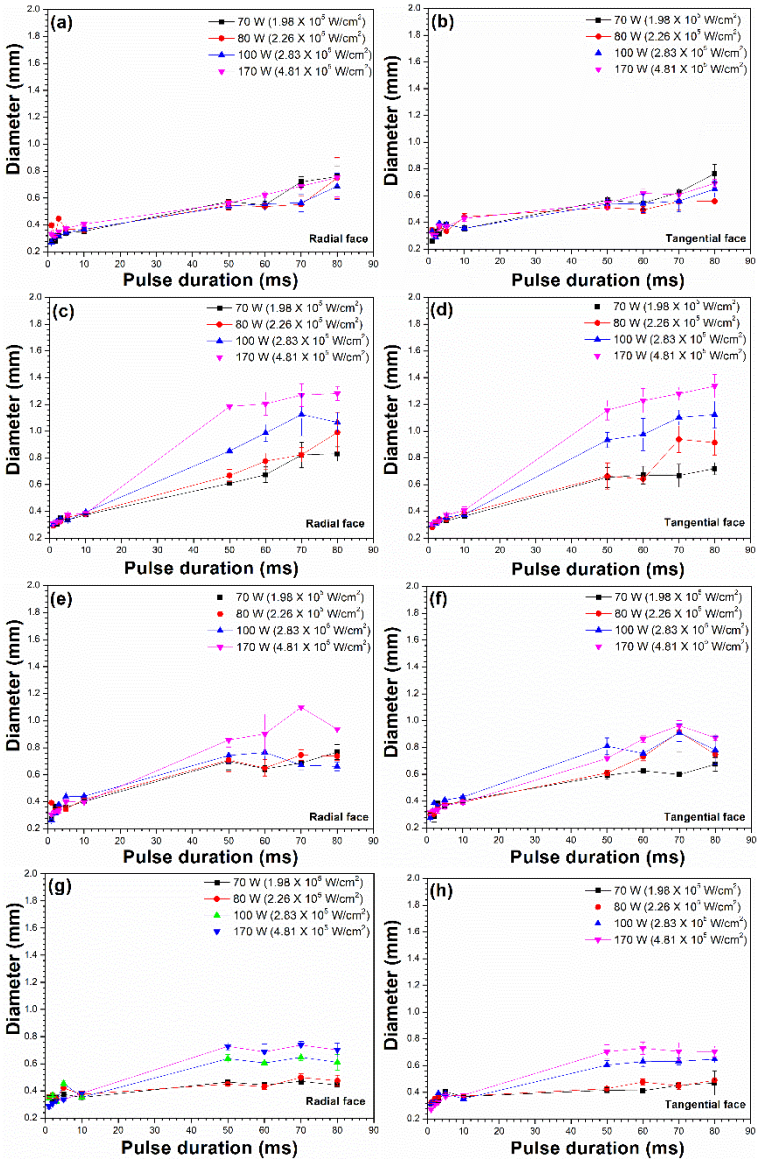

Figure 11 Effect of laser pulse duration on the diameter of the laser incised holes in (a, b) Southern Yellow Pine, (c, d) Radiata Pine, (e, f) European Redwood and (g, h) Beech. a, c, e and g represent the radial face and b, d, f and h represent the tangential face.

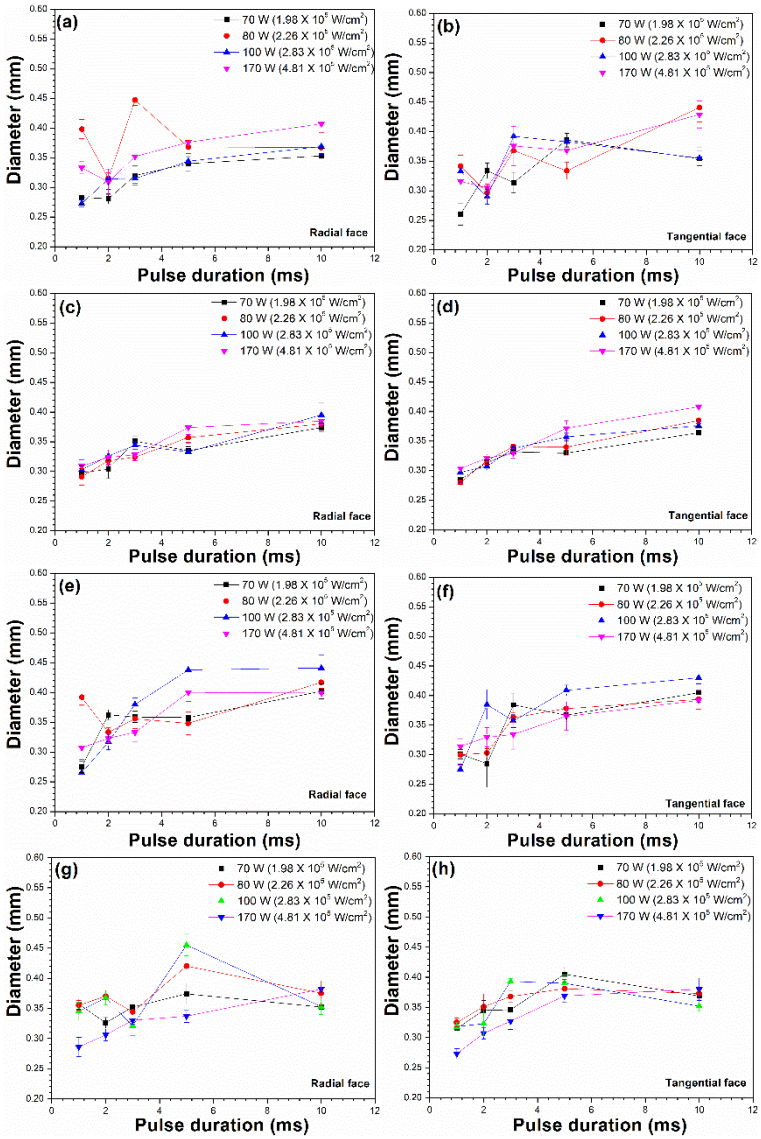

Figure 12 Effect of laser pulse duration on the diameter of the laser incised holes in (a, b) Southern Yellow Pine, (c, d) Radiata Pine, (e, f) European Redwood and (g, h) Beech. a, c, e and g represent the radial face and b, d, f and h represent the tangential face.

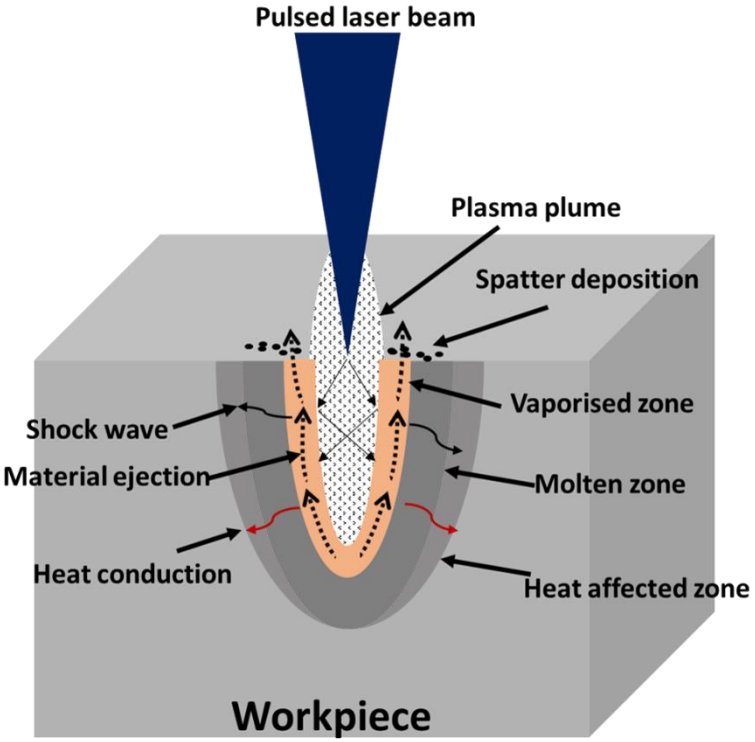

Figure 13 Schematic representation of laser interaction with the wood and associated effects.

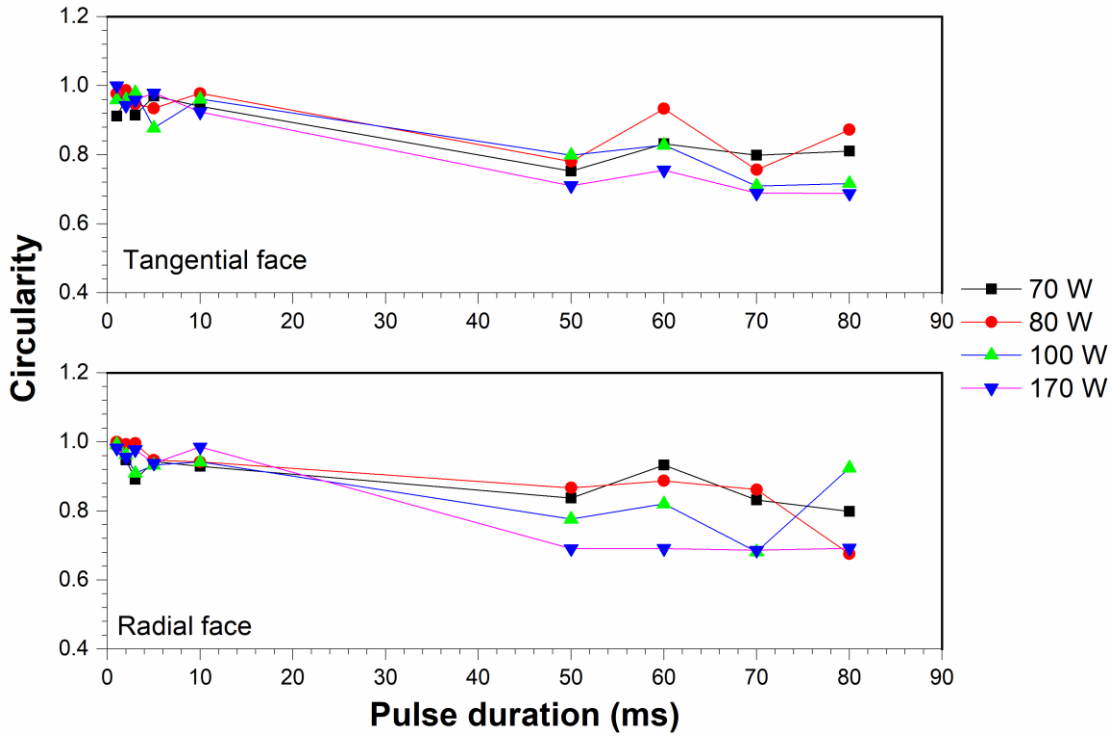

Figure 14 Effect of applied laser pulse duration on the circularity of laser incised holes in Southern Yellow Pine.

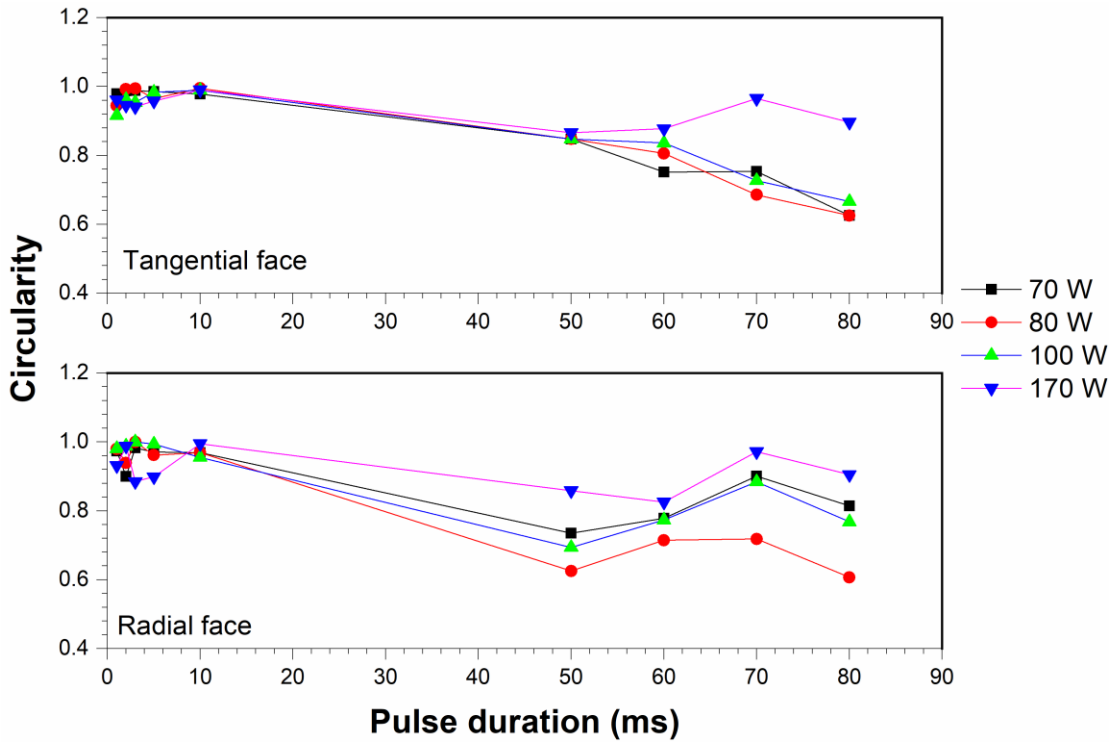

Figure 15 Effect of applied laser pulse duration on the circularity of laser incised holes in Radiata Pine.

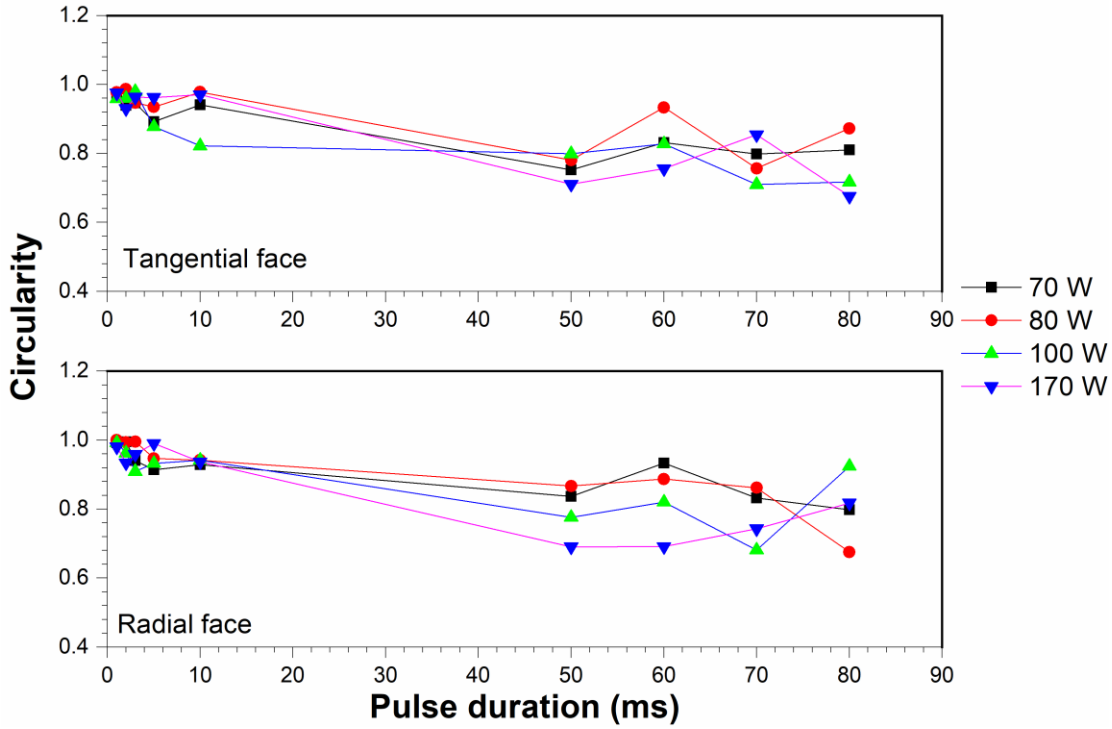

Figure 16 Effect of applied laser pulse duration on the circularity of laser incised holes in European Redwood.

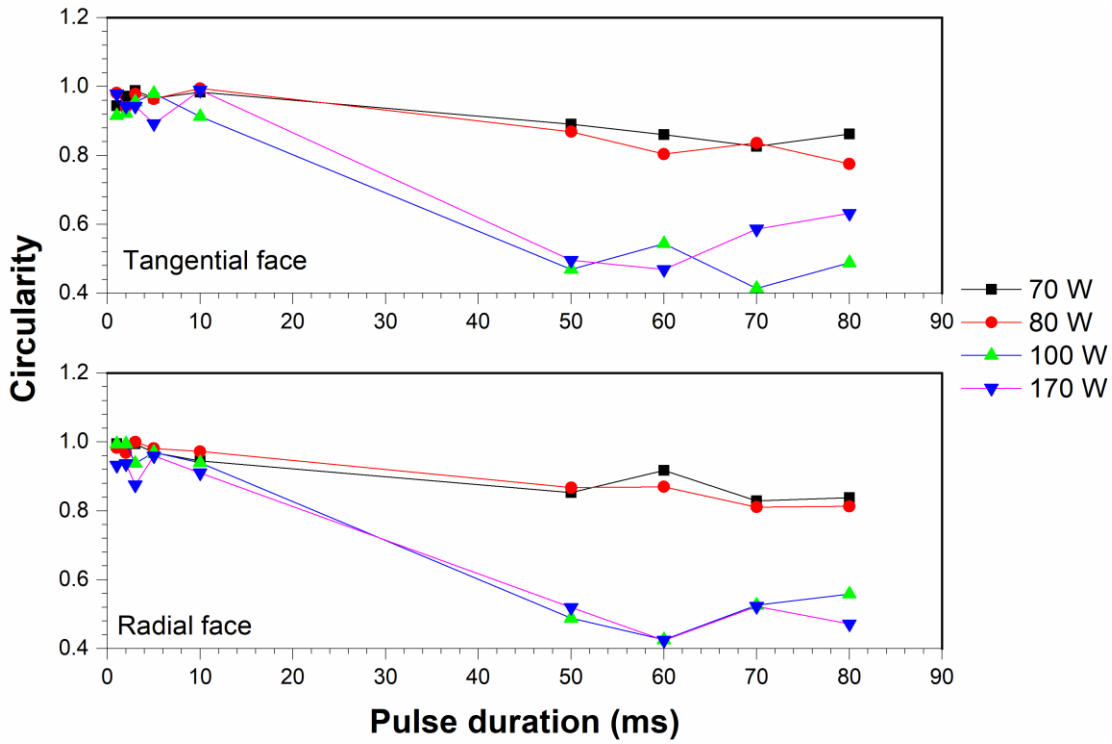

Figure 17 Effect of applied laser pulse duration on the circularity of laser incised holes in Beech.

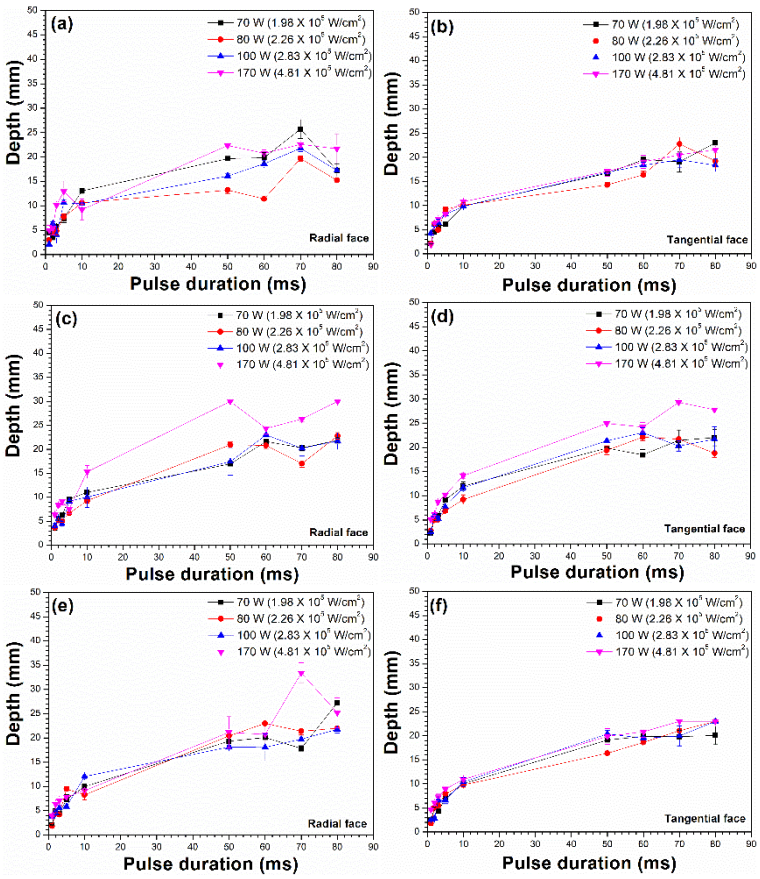

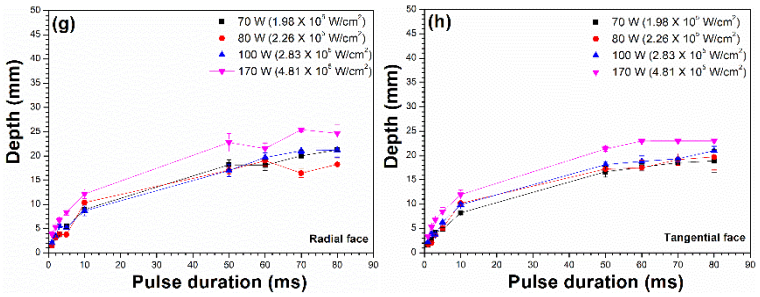

Figure 18 Effect of laser pulse duration on the depth of the laser incised holes in (a, b) Southern Yellow Pine, (c, d) Radiata Pine, (e, f) European Redwood and (g, h) Beech. a, c, e and g represent the radial face and b, d, f and h represent the tangential face.

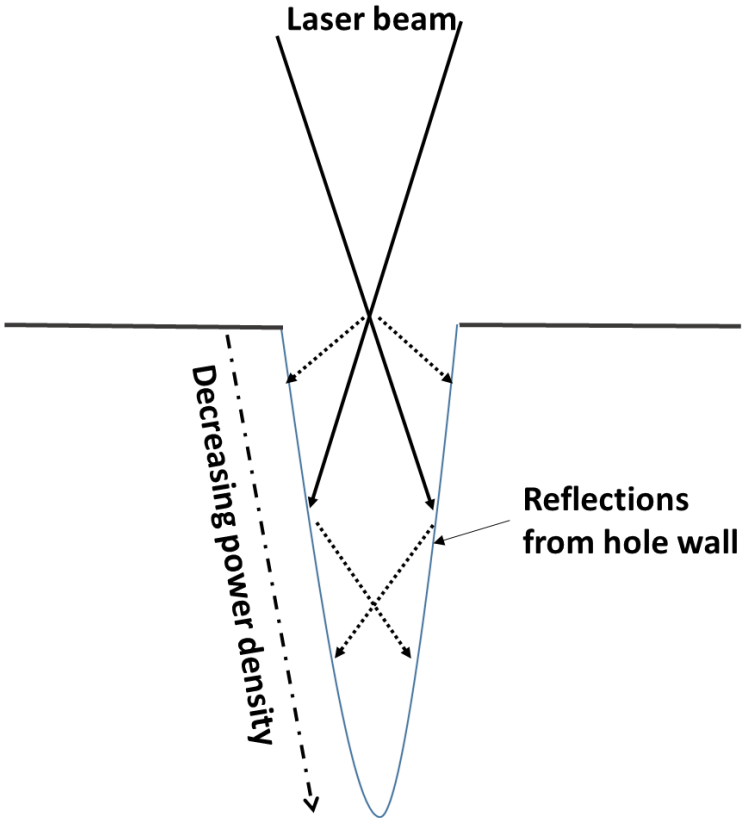

Figure 19 Variation of laser power density with depth.

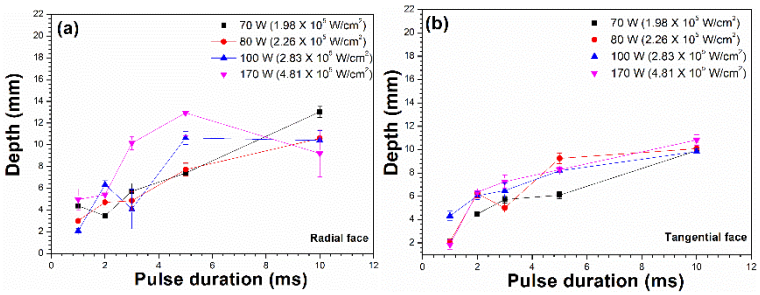

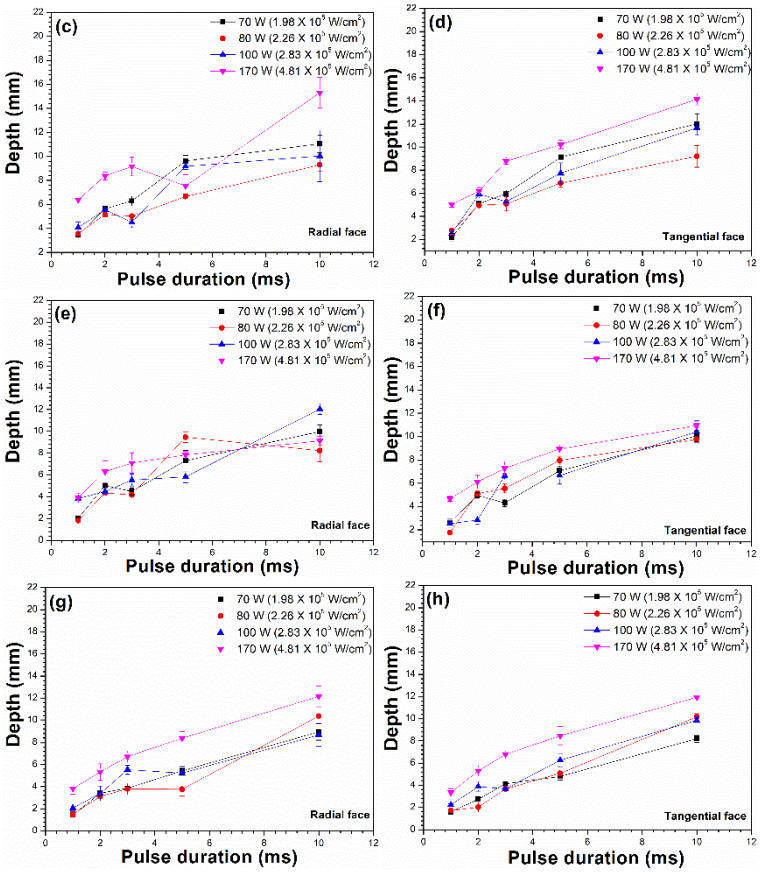

Figure 20 Effect of laser pulse duration on the depth of the laser incised holes in (a, b) Southern Yellow Pine, (c, d) Radiata Pine, (e, f) European Redwood and (g, h) Beech. a, c, e and g represent the radial face and b, d, f and h represent the tangential face.

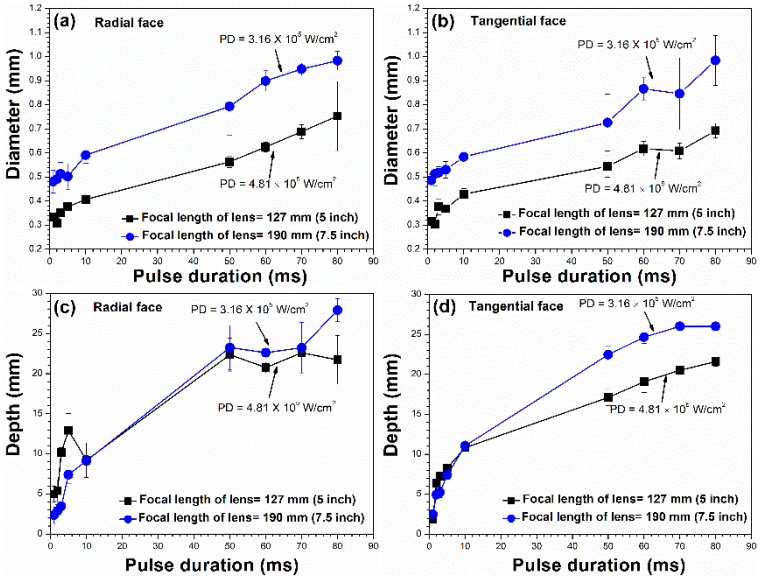

Figure 21 Effect of two different focal lengths on the (a,b) diameter and (c, d) depth of CO_2 laser incised holes, on the (a, c) radial and (b, d) tangential faces of SYP for an the applied laser power of 170 W.

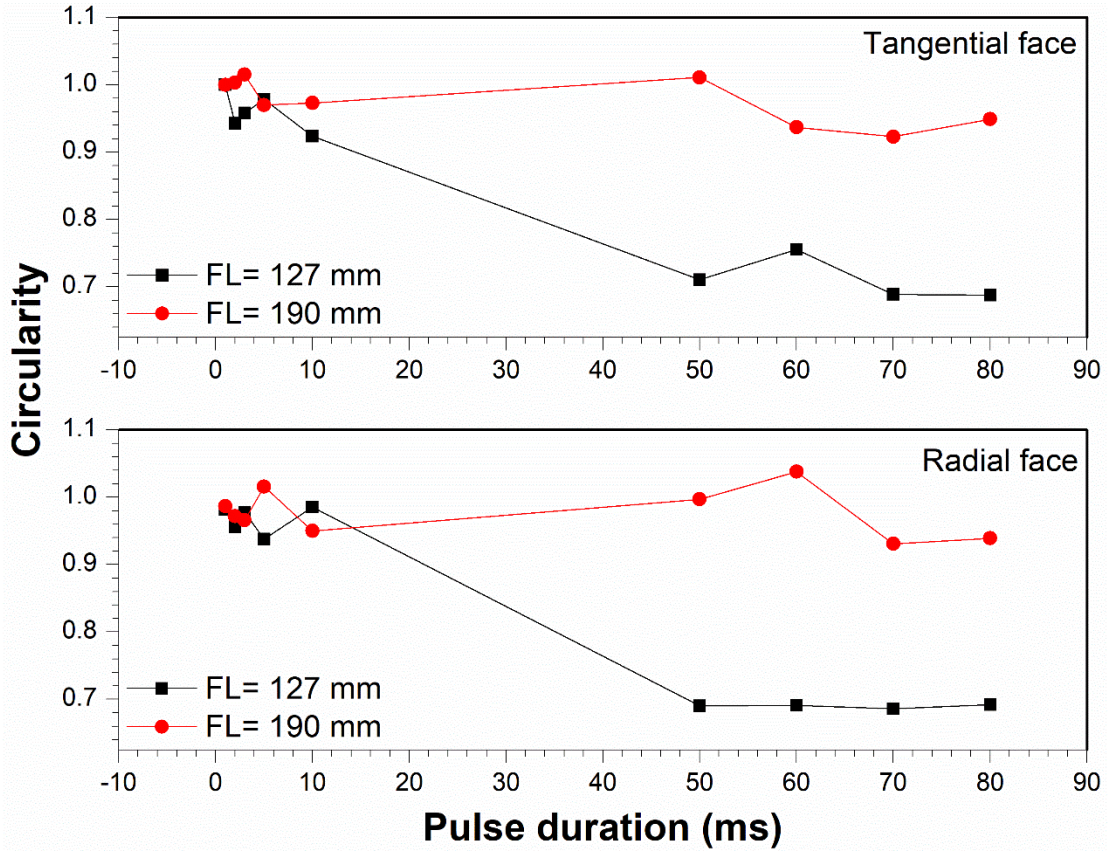

Figure 22 Effect of focal length of lens on the circularity of CO_2 laser-incised holes on the radial and tangential faces of the wood samples.

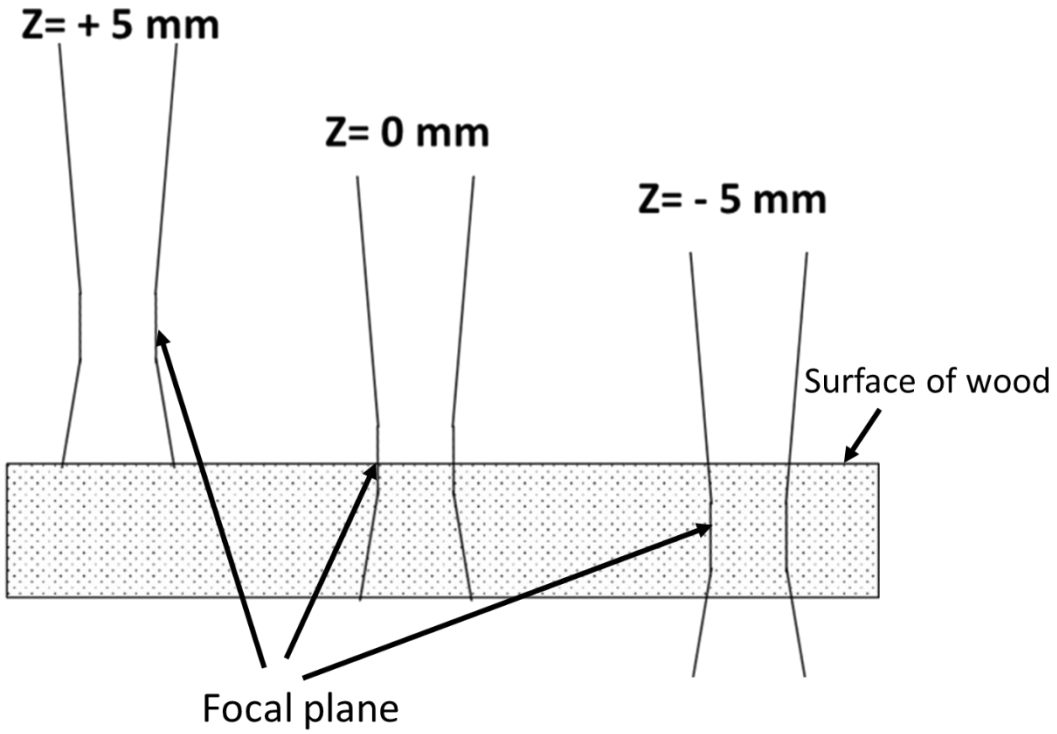

Figure 23 Schematic representation of focal point positioning during the laser-incision process.

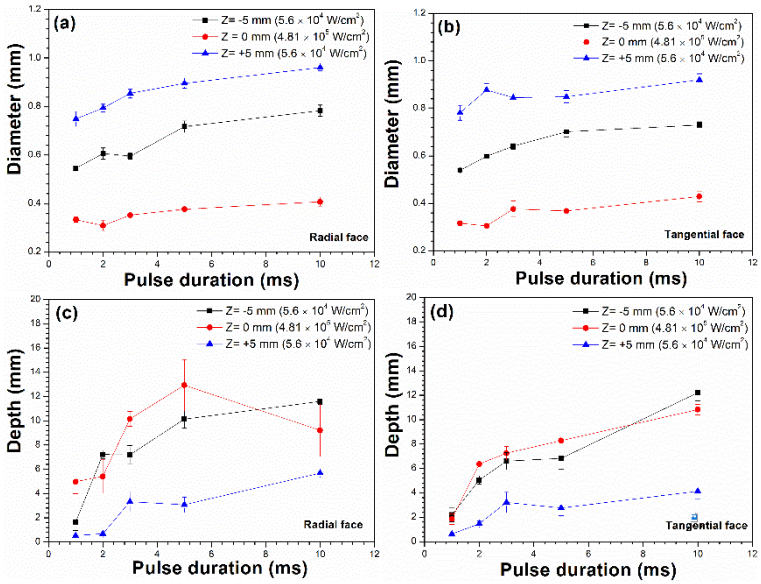

Figure 24 Effect of laser pulse duration on the (a, b) diameter and (c, d) depth of laser incised holes, on the (a, c) radial and (b, d) tangential faces of Southern Yellow Pine for a laser power of 170 W at different focal point positioning.

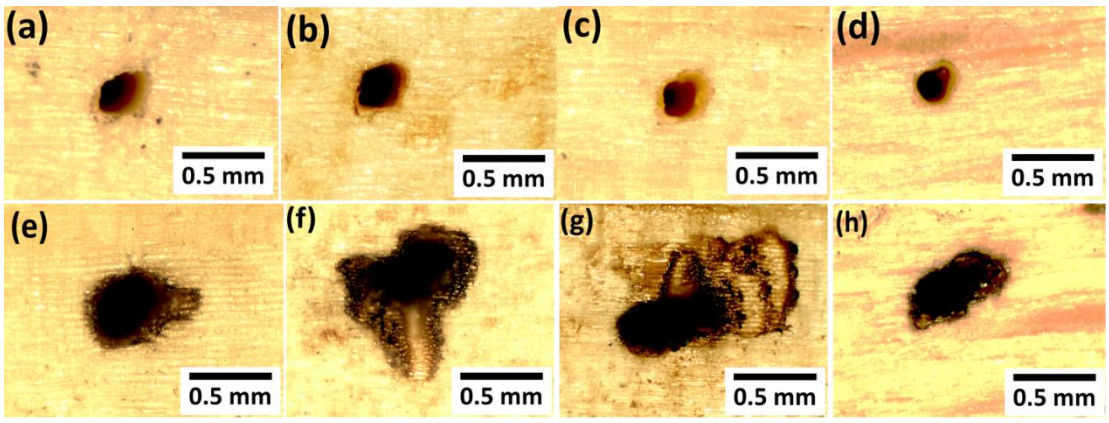

Figure 25 Optical micrographs showing diameter of laser incised holes with a laser power of 170 W and a pulse duration of 1 ms (a-d) and 80 ms (e-h) on the radial face of (a, e) Southern Yellow Pine, (b, f) Radiata Pine, (c, g) European Redwood and (d, h) Beech.

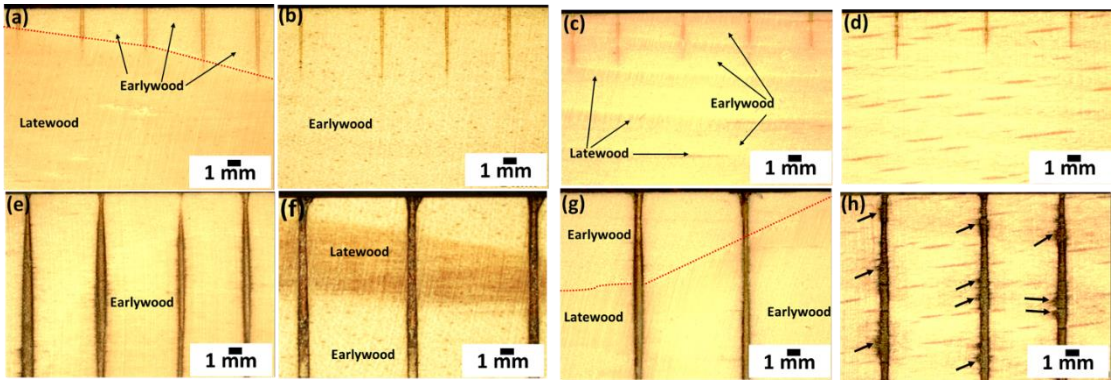

Figure 26 Optical micrographs showing depth of laser incised holes with a laser power of 170 W and a pulse duration of 1 ms (a-d) and 80 ms (e-h) on the radial face of (a, e) Southern Yellow Pine, (b, f) Radiata Pine, (c, g) European Redwood and (d, h) Beech.

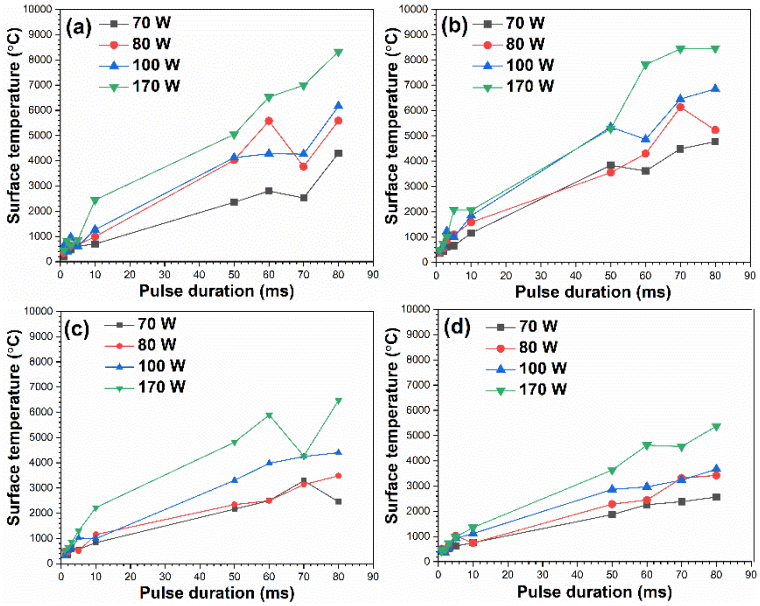

Figure 27 Variation of peak surface temperature during laser-perforation in (a) Southern Yellow Pine, (b) Radiata Pine, (c) European Redwood and (d) Beech during laser-perforation at different laser powers and pulse durations.

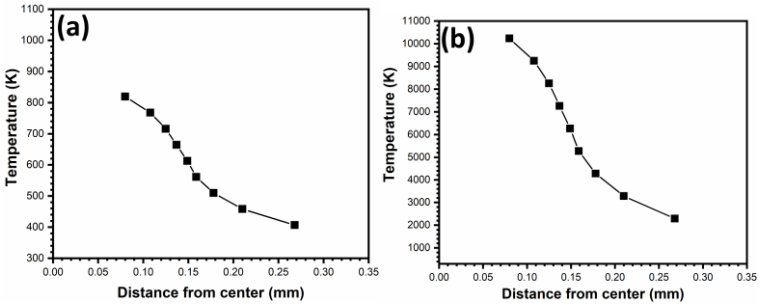

Figure 28 Finite element analysis of temperature rise on the surface of the wood at (a,b) a laser power of 70 W and a pulse duration of 1 ms and (c,d) a laser power of 170 W and a pulse duration of 80 ms.

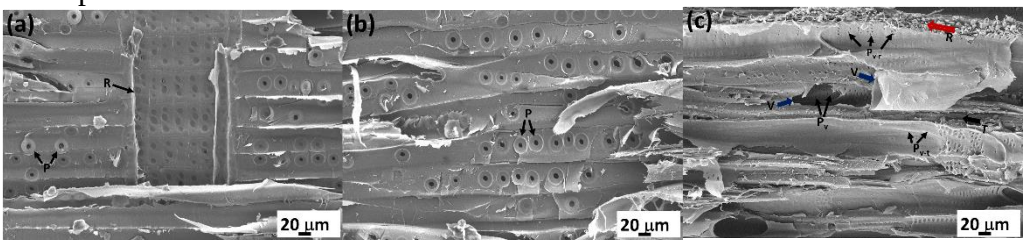

Figure 29 Scanning electron micrographs of unincised (a) Southern Yellow Pine, (b) Radiata Pine, and (c) Beech. (P= Pits; R= ray cells; T= tracheid; V= vessel; Pv= pits connecting vessel to vessel; Pv-r= pits connecting vessel to ray cells; Pv-t= pits connecting vessel to tracheid.)

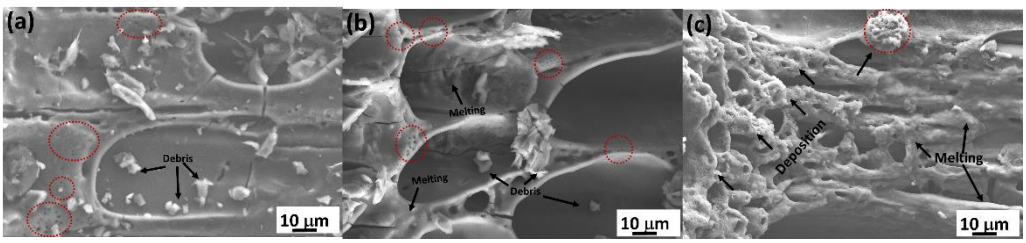

Figure 30 Scanning electron micrographs of laser incised regions in (a) Southern Yellow Pine, (b) Radiata Pine, and (c) Beech with a laser power of 170 W and a pulse duration of 80 ms.

List of Tables

Table 1: Physical and thermal properties of wood species used in the present study.

Species	Plank code	Moisture content (%)	Density (kg/m^3)	Specific heat capacity (J/kg K)	Thermal conductivity (W/m K)
Southern yellow pine	SYP	9.26	550	1546	0.144
Radiata pine	RP	7.92	400	1512	0.11
Redwood	RW	11.43	590	1599	0.154
Beech	BE	10.95	730	1588	0.185

Table 2: Laser-incision parameters used in the present study.

Parameters	CO_2 laser
Wavelength (μm)	10.6
Mode	Single-pulsed
Power (W)	70, 80, 100, 170
Pulse duration (ms)	1, 2, 3, 5, 50, 60, 70, 80
Pulse frequency	1Hz
Beam type	Gaussian
Raw beam diameter (mm)	20
Focused beam diameter (mm)	0.3 (for 127 mm) and 0.37 (for 190 mm)
Beam quality (M^2)	1.05
Focal length of lens (mm)	127 and 190
Shielding gas	No gas

Table 3 Comparison of theoretical beam diameter and depth of focus for two focal lengths.

Focal length of lens (mm)	Theoretical beam diameter at the focal plane (mm)	Depth of focus (mm)
127	0.086	0.54
190	0.128	1.22